Anatomically based cranial landmarks for three dimensional superimposition

by

Rongning Wu B.D.S., M.S.

Submitted in partial fulfillment of the requirements

for the degree of Master of Science in Dentistry

Thesis Advisor: Mark G Hans, D.D.S., M.S.

Case Western Reserve University

School of Dental Medicine

Department of Orthodontics

January 21, 2012

DEDICATION

To my parents, Gang and Yuehui, who sacrificed their life for their children, and continue to do so every day.

To my sister, Xiaohong, an architect who plans and designs the construction of buildings, yet keeps encouraging and inspiring me to be a dental architect.

ACKNOWLEDGEMENTS

I am sincerely thankful to my supervisor, Dr. Mark Hans, whose encouragement, guidance, and support from the initial to the final enabled me to develop an understanding of this subject. I am also grateful for your trust in accepting me into this orthodontic program which makes my dream come true. Many professors from China to United States have crossed my path in the long road to eventually becoming an orthodontist. You are someone I will nerve forget. Your engagement of science and art has inspired me to pursue a path of life-long learning. I am very proud of being your student.

My so many thanks to my committee members: Dr. Martin Palomo and Dr. Michael Landers for their support and advice throughout this process. Further your patience, forgiveness, and generosity have inspired me to meet the difficulties during this uneasy journey.

Many thanks to my honored committee member, Dr. Lysle Johnston, whose wikipedia-like knowledge, scientific thinking revamped my understanding of academia. I can honestly say you are someone I wish I could be.

Thank you to the faculty of Case Western Reserve University Department of Orthodontics. Your dedication and generosity have prepared the residents to be great orthodontists. I appreciate your effort to create the best learning experience.

ANATOMICALLY BASED CRANIAL LANDMARKS FOR THREE DIMENSIONAL SUPERIMPOSITION

Abstract

By

RONGNING (GRACE) WU

Objectives: The purpose of this study was to report the validity and reliability of identification of biologically relevant cranial-base landmarks using CBCT images of untreated orthodontic patients. **Methods:** Thirty CBCT images were selected randomly from the initial records of 743 patients ranging from 10-16 years. Optic foramina, foramina ovale and foramen cecum were defined and identified in the axial, coronal and sagittal plane respectively. Intra-examiner reliability was measured using the intra-class correlation coefficients for all landmark coordinates. The mean of the standard deviations (measures of dispersion), the error of the standard deviations (the estimating errors) were calculated for each landmark and each coordinate. Intra-class correlation was used to estimate reliability of location each landmark. **Results:** All of the measures of dispersion

were less than 0.3mm, ranging from 0.078 to 0.258mm. The variation of the estimates for the location of foramen cecum were greater along the horizontal (X) axis when compared to the vertical(Y) and anterior-posterior (Z) directions. Variations in the estimates of the location of the optic foramina were symmetrically distributed among the X, Y, and Z axis. Variations in the estimates of the location of foramina ovale were greater in the X axis compared to the Y or Z axes. Intra class correlations for all measures were 0.99. **Conclusions:** Foramina ovale, optic foramina and foramen cecum are acceptable landmarks for longitudinal superimposition on the cranial base.

TABLE OF CONTENTS

Page

DEDICATION.....i

ACKNOWLEDGEMENTS.....ii-iii

ABSTRACT.....iv-v

TABLE OF CONTENTS.....vi

LIST OF TABLES.....vii

LIST OF FIGURES.....viii

REVIEW OF THE LITERATURE.....1-20

LIT REVIEW REFERENCES.....21-23

MANUSCRIPT FOR PUBLICATION.....24-53

MANUSCRIPT REFERENCES.....54-55

APPENDICES.....56-63

1. IRB APPROVAL.....57
2. SAMPLE SIZE CACULATION 58
3. RAW DATA FOR FORAMEN CECUM COORDINATES.....59
4. RAW DATA FOR LEFT FORAMEN OVALE COORDINATES....60
5. RAW DATA FOR RIGHT FORAMEN OVALE COORDINATES...61
6. RAW DATA FOR LEFT OPTIC FORAMEN COORDINATES....62
7. RAW DATA FOR RIGHT OPTIC FORAMEN COORDINATES...63

LIST OF TABLE

Table I.-- Definition of the selected Landmarks for this study 40

Table II.-- Landmarks in X, Y, Z coordinate system.....41

LIST OFFIGURES

Figure 1.--Demonstration of biologically relevant anatomical structures.....42

Figure 2.--Demonstration of McRae's Line.....43

Figure 3.-- Fixing/registering head position in the coronal view.....44

Figure 4.-- Fixing/registering head position in the axial view.....45

Figure 5.-- Fixing/registering head position in the sagittal view.....46

Figure 6.-- Registering and recording the center of foramen cecum by the Invivo 5.0 software as numerical values for the X, Y, and Z coordinates respectively....47

Figure 7.--Registering and recording the center of left foramen ovale by the Invivo 5.0 software as numerical values for the X, Y, and Z coordinates respectively....48

Figure 8.--Registering and recording the center of right optic foramen by the Invivo 5.0 software as numerical values for the X, Y, and Z coordinates respectively....49

Figure 9.--Distribution of error for foramen cecum in the X, Y, and Z directions.....50

Figure 10. Distribution of error for foramina ovale in the X, Y, and Z directions.....51

Figure 11. Distribution of error for optic foramina in the X, Y, and Z directions.....52

Figure. 12. Demonstrations on distribution of error in the X, Y, and Z directions by using coronal, axial and sagittal views..... 54

REVIEW OF THE LITERATURE

In 1931, two-dimensional (2-D) cephalometric radiography was invented by Broadbent (Broadbent). The cephalometric method allowed comparison of serial lateral cephalograms using relatively stable structures in the cranial base, maxilla and mandible. Thus superimposition techniques allowed new discoveries about normal craniofacial growth and development as well as knowledge about the effects of orthodontic treatment on the teeth and bones. Although it has played a major role in orthodontics, 2-D superimposition had some inherent weaknesses. It compresses the three dimensional skull into a two dimensional shadow image. Therefore, 2-D cephalometry inevitably loses some information compared to the study of lifelike three dimensional (3-D) structures (M. G. Hans). In traditional cephalometry, 3-D craniofacial structures are projected onto 2-D radiographic film. This process creates a two-dimensional shadow of the three-dimensional object. Hans stated that these structures are effectively optical illusions of craniofacial anatomy (Hixon). He listed some examples of such structures which are the mandibular symphysis, the

pterygoid fossa, and the "key ridge." Although orthodontists constantly refer to these structures as anatomic landmarks, they are in fact, artifacts of the cephalometric technique. Another problem is that bilateral anatomical structures project a dual image on the radiograph and do not superimpose perfectly on the lateral cephalogram, because the fan of the x-ray beam diverges as it passes through the head. To compensate, clinicians average bilateral structures. An example of this process is the averaging of the right and left inferior borders of the mandible to create the "mandibular plane." Such averaging of bilateral structures creates two problems. First, the "plane" that is created is really now a line and is an abstraction based on the anatomy of the patient. Secondly, averaging the structures results in a loss of parasagittal information, and any true asymmetry of the patient is lost.

Another weakness of 2-D projection is the introduction of radiographic enlargement caused by nonparallel X-ray beams which originate from a small source. Early in 1960s, some pioneers had commented on these projectional errors. Hixon pointed out that the amount of chance error that

can be tolerated depends upon the purpose of the measurement taken (Hixon). Such errors, especially those errors arising from angular measurements, can usually be ignored in orthodontic diagnosis, as the magnitude of the error is very small in comparison to the size of the common facial measurements. Ahiqvist et al. examined the problem from a theoretical point of view and have concluded that projection errors in linear measurements are not a serious problem in cephalometry (Ahlqvist). However, the longitudinal study of normal facial growth requires high precision in measurement in order to investigate and interpret approximate true biologic changes from year to year. In order to minimize the systematic problems, Broadbent (Broadbent BH) introduced the Broadbent Orientator which used the information gained from biplane film radiographs to create 3D data points. Although this method is sound, it could not be widely employed due to its difficult application, and it yields less accurate measurements than true anatomic values (Grayson). Therefore, 3D data collection was not routinely attempted. Needless to say, longitudinal study based on various linear and angular measurements inevitably lost some information of geometry of the full

landmark configuration. And it is impossible to determine how important this lost information is to diagnosis and treatment planning.

At the end of the 20th century, Corn Beam Computed Tomography (CBCT) was implemented in dentistry and provided a one to one 3-D reconstruction of the entire cranial facial skeleton. (O'Higgins). CBCT uses a single 360° rotation of the x-ray tube around the head to acquire the images. Using this technology, the images are captured without critical concern of head position or object film distance. Errors of 2-D projection can arise because of variations in head position when radiographs are obtained. Broadbent had stressed that the importance of using a cephalostat to obtain and coordinate both frontal and lateral head films. In his article he first introduced the head holder. (Broadbent) The lateral and frontal radiographs are taken using two different x-ray sources positioned at right angles to each other. The patient's head is not moved between the exposure of the lateral and the frontal film. To insure standardized views of the patient's projected anatomy, it is important that only the source of the x-ray beam and the position of the film change between the exposures of the frontal

and lateral cephalogram images. This is a critical detail of the system because movement of the patient's head between exposures generates too much variation in the location of landmarks to make them clinically useful for 3D analysis. In contrast, CBCT is not as sensitive to variations in head position and therefore the use of a common reference plane to compare images is not as important. (Badawi-Fayad).

We expect superimposition of CBCT volumes to be a major source of new knowledge about normal craniofacial growth and to provide important new information about the effects of orthodontic treatment on craniofacial structures. , Most present studies focus on how to superimpose on 3-D models. Generally, there are two approaches to 3D superimposition: use of registration points or a mathematical algorithm. Registration points use a number of reference points that are registered on two volumetric images. Mathematical algorithm method, based on the probability and information theory, calculates the best fit of the two volumes of interest (VOI) and automatically superimposes the two volumetric images. No matter which method is employed, few studies have explored the feasibility of comparing our 2-D

superimposition knowledge to the three D world.

The vital concern is about 2-D landmarks.3-D superimposition needs relatively stable landmarks or structures to be superimposed on. The question here is whether conventional 2-D superimposition landmarks can be transitioned to 3-D. Location of 2D landmarks on the skull and the actual 3D CBCT model still poses a challenge. Dating back to stable structures for superimposition, several authors have stated that superimposition of 3D images could be an alternative method for analyzing changes during and after treatment. Oliveira et al. stated that this is challenging because of the difficulty of selecting stable areas or structures as registration points that would not change during orthodontic treatment. In 2-D superimposition, the American Board of Orthodontics (ABO) has adopted the cranial anatomical method by recommending registering "on the best fit of the anterior cranial base anatomy and center of sella turcica" (ABO). The ABO method is based on de Coster's observation of a stable basicranial line from the inner contour of the frontal bone to the anterior aspect of the sella turcica (Coster). However, the controversial viewpoint for conventional landmarks in

2-D superimposition has existed for a long time. Enlow and Hans pointed out that Sella and Nasion are not a true fixed and zero growth point (Hans and Enlow). Melsen (1974) commented that sella and nasion are not suitable stable longitudinal references which are consistent with the result from Bjork and Skieller (B. Melsen) (Bjork and Skieller). Baume and Bjork believed the remodeling of the sella turcicas during growth result in the position of the midpoint of sella turcicas being displaced backward and either upward or downward (Baume) (Bjork and Skieller). Although Sella turcica is used as gold referred landmark because sphenooccipital synchondrosis (SOS) is regarded as one of horizontal and vertical growth centers (Hans and Enlow) (Ricketts), unequal and asymmetric growth of SOS poses a problem for any growth pattern study based on sella turcica (Coben) (B. Melsen) (Baume) (B. Melsen). If sella's stability is doubtful, then validity of sella-nasion line is even more unreliable. Therefore sella-nasion has received much justified criticism as longitudinal reference by Ricketts and Ghafari. Another involved structure is anterior cranial base (ACB). If ACB is used in superimposition, it also ignores the contribution of the SOS' angular growth

relative to increases in distance between anterior and posterior cranial bases. Enlow and Hans believed that cranial base is not truly stable and unchanging. The floor of the cranium continues to grow and undergo remodeling changes throughout the childhood period (Hans and Enlow). If ACB is used in superimposition, it also ignores the contribution of the SOS' angular growth relative to increases in distance between anterior and posterior cranial bases. Thus, it is necessary to find new stable reference landmarks by means of 3-D reconstruction image. Otherwise, superimposition based on our bias regarding the "stability" of the reference landmarks inevitably produces unreliable results. If some relatively valuable structures can be found, it will contribute to draw a complete picture for actual changes and longitudinal growth patterns.

Consequently, the replacement of conventional superimposition with 3-D for the assessment of craniofacial relationships has the potential to be a significant step forward in orthodontic, since 2-D superimposition has its intrinsic insufficiency. Recently Case Western Reserve University Bolton-Brush center has been trying to develop a 3-D superimposition method to

compare results in pre- and post -treatment by means of CBCT. Since 3-D just started its baby step, 3-D superimposition available for routine craniofacial care still has long way to go. Basically there are four stages to establish a valid and reliable method. The first is to decide which potentially stable structures are worth testing based on 2-D study. The second is to define, identify and register these structures in the orientated head. The third one is to test the stability of these structures longitudinally using geometry method. The fourth is to superimpose 3-D images on those structures.

The aim of this study is to report the accuracy and reliability of identification of potentially stable cranial-base landmarks using CBCT images. In present study, foramina ovale, optical foramina and foramen cecum were selected to test. When approaching this research, we began with the questions: 1. why these structures were selected .2. How to define, identify and register them?

Although everything is changing over time, people have been attempting different methods to find relatively stable structures analyzing facial growth. Among those attempts, Bjork's method, using metallic radiographic markers, has obtained wide acceptance. Inspired by the

unchanging mandibular nerve canal during growth found by him, the assumption that some cranial nerves remained unchanging after certain period of time was brought up. Since optical foramina and foramina ovale both seated in sphenoid bone, the relatively mutual position of these structures in one bone was stable. What's more, these structures were influenced least after the brain size was almost complete at the age of 5 years (B. Melsen). Although the cranial structures underwent lifelong surface remodeling, whether the inner surface of nerve canals have experienced the same changes is doubtable. If yes, the patients have more chances to suffer some neuronal symptoms.

Houston in 1983 pointed out that many cephalometric landmarks in 2-D have been defined for convenience of identification and reproducibility, rather than on grounds of anatomic validity (Houston). And Bookstein mentioned that there is a lack of literature about suitable operational definitions for the 2-D traditional landmarks in the 3 planes of space (coronal, sagittal, and axial) (F. Bookstein). Therefore, to define the valid anatomical cranial structures used for present study is not trivial.

In Hodaie's study, the optic nerve included prechiasmatic portion, chiasm, retrochiasmatic tract, and optic radiation. Anatomically, we selected the prechiasmatic portion of optic nerve was selected to define the optic nerve Based on his study (Hodaie). Radiographically, the prechiasmatic portion in present study is the nerve starting from chiasmatic groove to 3.8-4mm forward in sagittal and axial view. Berlis recommended that the best observation of optical foramina is in coronal view. Once sagittal and axial view were adjusted properly, it was easy to register the center of optical foramina in coronal plane (Berlis).

In Berlis' study, he suggested that it is optimal to observe foramen ovale in the axial projection in which they are presenting the circular shape of ovlae (Berlis). Radiographically, in sagittal view, the middle portion of an opening between the anterior wall which locates in the most posterior-superior part of lateral pterygoid process and posterior wall which visibly locates in the opposite side. In coronal view, the middle portion between the lateral and inner wall of the opening of sphenoid bone. Once sagittal and coronal view were adjusted properly, it is easy to register the center of foramina ovale in axial

plane.

Theoretically, head orientation should not be the imperative concern in 3-D superimposition for eliminating the errors of measurement. However, in present study, cross-sectional slices instead of 3-D rendering in three planes were used for registration of landmarks, because 3D renderings are projected images and not actual surfaces. And since single cross-section of a larger structure is viewed, small variations in head positioning corresponds to large changes in the cross-section view. In 2-D study, Broadbent's classic cepholostat used external cranial structures including the external auditory meatus, Frankfort horizontal plane, and nasion, to orientate the head. Since 3-D provides clinicians with the ability to investigate the inner depths of the human anatomy slice by slice, in present study, optical foramina, foramina ovale, basion, opisthion and foreman cecum are selected based on the assumption that these internal cranial structures are not altered after treatment and relatively stable compared with external cranial structures. More importantly, because we're viewing single cross-sections of a larger and longer structure, small variations in head positioning

corresponds to large changes in the cross-section view. Without correcting for the positioning, it is difficult to determine the cause of changes in a CBCT cross section of two separate images of the same subject as the images may not be comparable. The selection of cranial base was due to its lack of tendency for growth and change. Friede reported that cranial base is relatively stable during growth since the brain size and volume have achieved more than 85% of its total size at the age of 5 (Friede). By selecting stable structures within this region, a protocol needs to be created allowing us to reach the same orientation of the head reliably. After reaching a reliable orientation, we are then able to use single reference points for comparison instead of needing to define multiple points of a structure in multiple dimensions in order to correct for changes. A single point now will yield similarly corresponding coronal, sagittal, and axial plane CT images. In comparison to the 2-D, the internal cranial landmarks were chosen to position the head in this study including optic foramen, foramen ovale, foramen magnum and foramen cecum. These structures were selected based on two reasons: validity and reliability.

Validity has to be considered at both of what is measured and method of measurement. In 2-D superimposition, the validity of using sella and nasion as anterior cranial base are questionable. And validity of measuring them is in question as well. Many cephalometric landmarks have been defined for convenience of identification and reproducibility, rather than on grounds of anatomic validity. In cephalometric radiography, it is usually assumed that the midsagittal plane of the head is parallel to the plane of the film in lateral views and perpendicular to it in posteroanterior views. This depends on the ear-rod axis being perpendicular to the midsagittal plane of the head, an assumption that is often incorrect because of faulty positioning of the head in the cephalostat or anatomic variation in the position of the external acoustic meati. While small rotations do not severely distort lateral skull views, they can lead to a misleading diagnosis of asymmetry from posteroanterior views. In contrast, 3-D can minimize the small rotation by aligning the landmarks respectively in sagittal, coronal and axial views. Therefore, the head is allowed to orientate relatively precise over a period of time. In present study, foramen

optic, ovale, magnum and cecum were selected based on the assumption that these internal cranial structures are relatively stable over time compared with external cranial structures. What's more, 3-D provides a feasible method to adjust the selected landmarks in different views. Consequently, establishing a head position in 3-D is not an assumption but real execution.

Reliability is the consistency of a set of measurements. In 2-D, Several studies on the reliability of cephalometric landmarks have been published, and these provide guidance on the selection of landmarks. Baumrind employed 25 residents to register some landmarks (Baumrind and Frantz). He found that each landmark usually has noncircular envelope of error. Sella, the visual estimation of the center of a structure, is surprisingly precise. Inspired by Baumrind's study, structures presenting ovoid or round circles in different views were selected. It is assumed that the registration of center of circle might be easier and more precise.

Historically, landmarks, such as Articulare, were used because of the ease in landmark location on the 2D cephalometric projections, but these projected superimposed structures do not exist in the actual 3D

facial structure. For these reasons, the development of 3D landmark-based cephalometric analysis demands suitable operational definitions of the landmark location in each of the 3 planes of space, and reproducibility of landmark identification is necessary to take full advantage of the 3D diagnostic power offered by CBCT imaging. However, the development of 3D landmark-based cephalometric analysis requires definition of 3D landmarks on complex curving structures, which is not a trivial problem. As Bookstein noted, there is a lack of literature about suitable operational definitions for the landmarks in the 3 planes of space (coronal, sagittal, and axial) (F. Bookstein).

Anatomically, the optic foramen is the opening to the optic canal which is the superior surface of the sphenoid bone bounded behind by a ridge. Hodaie reconstructed and imaged the cranial nerves by Diffusion-based tractography (Hodaie). The prechiasmatic portion of optic nerve was selected to define the optic nerve Based on his study. He used 4 patients' MRI scan to reestablish 11 pairs of cranial nerves. In his paper, the optic nerve included segments spanning the prechiasmatic portion, chiasm, retrochiasmatic tract, andoptic radiation. The

prechiasmatic portion in present study is the nerve starting from chiasmatic groove to 3.8-4mm forward. Optic foramina were selected to align up the head in coronal view in order to prevent the lateral tilt of head. Methodologically, the coronal projection of the optic canal proved to be ideal for CT examination (Berlis). Berlis and his coworkers used 60 adult European skulls to compare cranial osseous structures using CT and direct measurement on skull. The conclusion showed the correlation of direct measurements with CT measurements of optic foramina were good. What's more he pointed out that the optical foramina present the "keyhole" character in coronal view.

In anatomy, Foramen ovale is situated at posterior border of great wing of sphenoid bone. In Berlis' study, he suggested that it is optimal to observe foramen ovale in the axial projection in which they are presenting the shape of truly ovlae 56.7%, an elongated ovlae 31.7%, or semicircular 11.7% (Berlis). The third branch of trigeminal nerve, mandibular nerve, goes through the foramen ovale. And the earliest perfect ring-shaped formation of the foramina ovale was observed in the 7th fetal month and the latest in 3 years after birth.

Therefore Foramina ovale were chosen to align up the head in axial plane to prevent the rotation of head.

Neurologically, McRae's line is defined by the opening of the foramen magnum. McRae’s line is the foramen magnum line drawn from the anterior margin of the foramen magnum (basion) to the posterior border (opisthion). McRae’s lines illustrate the degree of deformity and aid surgical decision making with regard to fixation and stabilization (Goel). Goel in 2004 reclassified the Type I and II basilar invagination -in which the odontoid process invaginated into the foramen magnum and the tip of the odontoid process was above the Chamberlain, McRae foramen magnum, and Wackenheim clival (Goel). Practically, it is easy to find MacRae’s line and align it up in sagittal image to prevent superior and inferior tilt of head. In fact, foramen magnum can be regarded as the biggest nerve foramen which the spinal cord goes through it. Little data are to be found concerning the absolute or relative growth of the sphenoid bone, the length of the pre-and post-sella portions of this bone are fairly stable at five years of age. Björk reported that the cranial base angle gradually bends in the first years of childhood up to about 10 years, but others have shown that bending

probably happens earlier in life, perhaps by 5 to 6 years or even 2 to 3 years (Bjork A and Skieller).

The frontal crest of the frontal bone ends below in a small notch which is converted into a foramen, the foramen cecum, by articulation with the ethmoid. This foramen varies in size in different subjects, and is frequently impervious; when open, it transmits a vein from the nose to the superior sagittal sinus.

Foreman cecum is a blind foramen formed immediately anterior to the crista galli by a notch at the lower end of the frontal crest and its articulation with the ethmoid bone. It is insignificant postnatally, but gives passage to vessels during development. In order to bisect the cranial base on the sagittal plane, a line was drawn which passes through foramen cecum in an anterior-posterior direction. This anterior-posterior line is drawn to be perpendicular to the medial-lateral line which passes through both of the foramen ovale.

It’s well known that errors in landmark affect the reliability of 2-D measurements. So inevitably 3-D will have the similar errors since cross-sectional slices instead of true 3-D rendering were used for registration of landmarks. Further, although structures were

identified in three planes using defined landmarks, there is still some ambiguity when anatomic structures were located. Therefore there is a need to quantitate the accuracy and precision of 3-D landmarks measurements. The aim of the present study is to report the accuracy and reliability of identification of cranial-base landmarks using CBCT images.

LIT REVIEW REFERENCE

Baumrind, Sheldon and Robert C. Frantz. "The reliability of head film measurements:1. Landmark identification." American Journal of Orthodontics (1971): 111-127.

ABO. American Board of Orthodontics. Case report preparation: composite tracings. St Louis, Mo, 2007.

Ahlqvist, J. "The effect of projection errors on cephalometric length measurements." European Journal of Orthodontics (1986): 141-148.

Badawi-Fayad. "Multi-detector row CT scanning in Paleoanthropology at various tube current settings and scanning mode." Surg Rodiol Anat (2005): 27(6):536-43.

Baume, LJ. "Principles of cephalofacial development revealed by experimental biology." Am J Orthod (1961): 47:881–901.

Berlis, A. "Direct and CT measurements of canals and foramina of the skull base." British Institute of Radiology (1992): 653-661.

Bjork , A and V Skieller . "Normal and abnormal growth of the mandible. A synthesis of longitudinal cephalometric implant studies over a period of 25 years." . Eur J Orthod (1983): 5:1–46.

Bjork A, A. and V. Skieller . "Facial development and tooth eruption: An implant study at the age of puberty." Am J Orthod (1972): 62: 339-383.

Bookstein , FL. "Morphometric tools for landmark data." Cambridge: Cambridge University Press (1991): 435.

Bookstein, Fred L. "Shape and the information in medical images: a decade of the morphometric synthesis." Computer Vision and Image Understanding (1997): 97-118.

Broadbent BH, Broadbent BH Jr., Golden W. Bolton Standars of Dentofacial Development. St.Louis,Mo: CV Mosby, 1975.

Broadbent. "Broadbent BH 1931.A new x-ray technique and its application to orthodontia, the introduction of cephalometric radiography." Angle orthod. (Reprint 1981): 51:93-114.

Broadbent, BH. Bolton Standars of Dentofacial Developent. St.Louis,Mo: CV Morby, 1975.

Coben , SE. "The spheno-occipital synchondrosis: the missing link between the profession's concept of craniofacial growth and orthodontic treatment." Am J Orthod Dentofacial Orthop (1998): 114:709– 712; Discussion 713-704.

Coster. "studied by a new line of reference." Trans Cong (28th) Eur Orthod Soc (1952): 50-5.

De Oliveira, Ana Emilia F. "Observer Reliability of Three-Dimensional Cephalometric Landmark Identification on Cone-Beam CT." Oral Surg Oral Med Oral Pathol Oral Radiol Endod (2009): 256-265.

Friede, Hans . "Normal Development and Growth of the Human Neurocranium and Cranial Base." Journal of Plastic and Reconstructive Surgery and Hand Surgery (1981): 163-169.

Goel, A. "Treatment of basilar invagination by atlantoaxial joint distraction and direct lateral mass fixation." J Neurosurg Spine (2004): 281-286.

Grayson, B. "The three dimentinal cephalogram, theory, technique and clinical application." Am J Orthod Dentofacial Orthop (1988 Oct;): 94(4):327-37.

Hans, M G. "Three-Dimensional imaging: The Case Western Reserve University Method." Semin Orthod (2001): 7:233-243.

Hans, Mark G and Donald Enlow. Essentials of Facial Growth. W.B. Saunders Company, 2008.

Hixon, E H. "Cephalometrics and longitudinal research." American Journal of Orthodontics (1960): 36-42.

Hodaie, M. "In vivo visualization of cranial nerve pathways in humans using diffusion-based tractography." Neurosurgery (2010): 795-796.

Houston, W.J.B. "Sources of error in measurements from cephalometric radiographs." European Journal of Orthodontics (1986): 149-151.

Melsen, B. The cranial base: the postnatal development of the cranial base studied histologically on human autopsy material. Copenhagen: Arhus., 1974.

Melsen, B. "The postnatal growth of the cranial base in Macaca rhesus analyzed by the implant method." Tandlaegebladet (1971): 75:1320–1329.

Melsen, Birte. "The postnatal development of the palatomaxillary region studied on human autopsy material." American Journal of Orthodontics (1982): 329-342.

O'Higgins. "Ontogeny and phylogeny: morphometric approaches to the study of skeletal growth and evolution." Chaplain MAJ, Singh GD, McLachlan J. John Wiley and Sons. On Growth and Form: Spatio-temporal Patterning in Biology. 1999. 373-393.

Palomo, J. Martin. "clinical application of three-dimensional cranialfacial imaging in orthodontics." Journal Medical Science (2005): 269-278.

Ricketts , RM. " New perspectives on orientation and their benefits to clinical orthodontics—part II." Angle Orthod (1976): 46:26–36.

Anatomically based cranial landmarks for three dimensional superimposition

Authors: Rongning (Grace) Wu B.D.S., M.S. [1]

Mark Hans, D.D.S., M.S.D. [2]

J. Martin Palomo, D.D.S., M.S.D. [3]

1. Resident, Department of Orthodontics at Case School of Dental Medicine in Cleveland, OH
2. Professor and Chair, Department of Orthodontics at Case School of Dental Medicine in Cleveland, OH
3. Associate professor and Program Director, of Orthodontics at Case School of Dental Medicine in Cleveland, OH

Corresponding Author:
J. Martin Palomo, D.D.S., M.S.D.
Case Western Reserve University
School of Dental Medicine
Department of Orthodontics
10900 Euclid Ave.
Cleveland, OH 44106

AMERRICAN JOURNAL OF ORTHODONTICS & DENTALFACIAL ORTHOPEDICS

MANUSCRIPT DRAFT

Title: Anatomically based cranial landmarks for three dimensional superimposition

Article Type: Original article

Keywords: Cone beam computed tomography, superimposition, head position, validity and reliability

Abstract:
Objectives: The purpose of this study was to report the validity and reliability of identification of biologically relevant cranial-base landmarks using CBCT images of untreated orthodontic patients. **Methods**: Thirty CBCT images were selected randomly from the initial records of 743 patients ranging from 10-16 years. Optic foramina, foramina ovale and foramen cecum were defined and identified in the axial, coronal and sagittal plane respectively. Intra-examiner reliability was measured using the intra-class correlation coefficients for all landmark coordinates. The mean of the standard deviations (measures of dispersion), the error of the standard deviations (the estimating errors) were calculated for each landmark and each coordinate. Intra-class correlation was used to estimate reliability of location each landmark. **Results:** All of the measures of dispersion were less than 0.3mm, ranging from 0.078 to 0.258mm. The variation of the estimates for the location of foramen cecum were greater along the horizontal (X) axis when compared to the vertical(Y) and anterior-posterior (Z) directions. Variations in the estimates of the location of the optic foramina were symmetrically distributed among the X, Y, and Z axis. Variations in the estimates of the location of foramina ovale were greater in the X axis compared to the Y or Z axes. Intra class correlations for all measures were 0.99. **Conclusions:** Foramina ovale, optic foramina and foramen cecum are acceptable landmarks for longitudinal superimposition on the cranial base.

INTRODUCTION

In 1931, two-dimensional (2-D) cephalometric radiography was invented by Broadbent.[1] One important contribution of cephalometrics to clinical orthodontics was the ability to compare serial cephalograms using relatively stable structures in the cranial base, maxilla and mandible. Such superimposition techniques allowed new discoveries about normal craniofacial growth and development as well as knowledge about the effects of orthodontic treatment on the teeth and bones. Although it has played a major role in orthodontics, 2-D superimposition had some inherent weaknesses. It compresses the three dimensional skull into a two-dimensional shadow image.[2] Therefore, 2-D cephalometry inevitably loses some information compared to the study of lifelike three dimensional (3-D) structures. In fact, some cephalometric features such as the mandibular symphysis, the pterygoid fossa, and the "key ridge" are effectively optic illusions of craniofacial anatomy.[3] Another limitation of the cephalometric technique is the bilateral anatomical structures project a dual image on the radiograph and do not superimpose perfectly because the x-ray beam diverges as it passes through the head. To compensate, clinicians average bilateral structures such as the right and left inferior borders of the mandible to create the "mandibular plane." Averaging of bilateral structures creates two problems. First, the "plane" that is created is really a line and is an abstraction based on the anatomy of the patient. Second, averaging the structures results in a loss of parasagittal information, and any true asymmetry of the patient is lost.[3] A third limitation of projection radiography is the enlargement of the image created by variations in object film distance.[2] The latter

limitation results in problems comparing linear measures taken on serial radiographs. Although there are several ways to correct for magnification errors, these are usually not applied in clinical settings and sometimes not even addressed in clinical research studies.[4,5] Therefore, although cephalometric radiography has increased our understanding of the growth process and the effects of orthodontic therapy, much remains to be learned.

Cone Beam Computed Tomography (CBCT) provides a three-dimensional (3-D) image of the entire cranial-facial skeleton using more than 300 2-D images captured by a flat x-ray sensor during a 360 degree rotation around the patients head.[6] The use of 3-D CBCT imaging in orthodontics is steadily increasing and the need for a method to compare longitudinal images has reached a critical level. It must be remembered that the big impact of traditional 2-D cephalometrics to orthodontics was not in describing craniofacial morphology, the real value of cephalometrics was the ability to compare longitudinal changes that occurred during growth and treatment. And, the knowledge gained from longitudinal studies did impact diagnosis and treatment planning. Similarly, 3-D superimposition will play a major role in furthering our understanding of how the face grows and the effects of orthodontic treatment on the growth process.

Longitudinal study requires a method to orient the serial images on relatively stable landmarks that can be seen on the image. For 2-D cephalometrics, Björk's classic implant studies provide the best data to identify the most stable structures for superimposition.[7] For 3-D we do not have any longitudinal implant studies. Generally,

there are two approaches to 3-D superimposition: use of registration points or use of a mathematical algorithm. The registration point method requires a human operator to identify a number of anatomical features that are visible in the two volumes images. The x, y and z coordinates of these features are gathered and a mathematical best fit of the coordinates produces the superimposition position for the volumes. The mathematical algorithm method uses probability and information theory to calculate the best fit of the two volumes of interest (VOI) based on density and location of the voxels within the image. The two volumes are then superimposed based on the voxel data. Most attempts at superimposition of CBCT craniofacial images have used the registration method. However, the question of what anatomic features should be used for registration has not been investigated. Based on our experience with cephalometric superimposition it would be helpful to superimpose serial CBCT images on the cranial base, the maxilla and the mandible. In addition the reliability of locating these anatomic features they should also be biologically relevant. Therefore, the aim of the present study is to report the validity and reliability of identification of biologically relevant cranial-base landmarks using CBCT images of untreated orthodontic patients.

MATERIAL AND METHOD

Thirty images were randomly selected from the initial records of 743 patients treated in XXX. The inclusion criteria for enrollment in present study were: Age between 10 and 16 years. Landmarks of measured structures can be seen clearly on the CBCT images. The exclusion criteria were: 1) no previous neurosurgery 2) no craniofacial deformities (syndrome) 3) non-cranial tumor based on medical history form 4) no previous orthodontic treatment based on medical history form. This study was approved by the XXX Institutional Review Board. And informed consent and Health Insurance Portability and Accountability Act (HIPAA) authorization forms were signed by all subjects.

All CBCT scans were taken in XXX using a field of view large enough to capture the craniofacial complex (CB MercuRayTM, Hitachi Medical Systems America Co. – Twinsburg, OH). The lowest mill amperage setting of 2mA was used. These settings resulted in a voxel size of 0.38mm. The reconstructed DICOM images were transferred to a commercially available software package that identified the x, y, and z coordinates of the cursor as it was placed by the operator over each anatomic feature of interest. (Invivo 5.0 Anatomy software).

Five biologically relevant anatomical structures and one line (plane) were identified during discussions with anatomists and experienced cephalomatricians (Table 1). The rationale for including each of these structures follows.

The optic foramina are bilateral structures are located in the sphenoid bone. The optic nerve along with the ophthalmic artery passes through these structures. The

center of the foramen as it enters the sphenoid bone is found by visual inspection and the x, y and z coordinates recorded (Fig. 1.).

The foramina ovale are also bilateral structures located in the posterior and lateral portion of the sphenoid bone. The center of the foramina as it enters the sphenoid bone is found by visual inspection and the x, y and z coordinates recorded (Fig. 1.).

The foramen cecum is a midline structure located where the frontal bone articulates with the ethmoid bone. The center of the foramen as it enters the sphenoid bone is found by visual inspection and the x, y and z coordinates recorded (Fig. 1.).

McRae's Plane is located in sagittal view and is defined as a line drawn from the anterior margin of the foramen magnum (basion) to the posterior border (opisthion) (Fig. 2.). McRae's line (or plane) is commonly used in neurosurgery as a stable reference for orienting the head in the sagittal plane. It also illustrates the degree of deformity and aids in surgical decision making with regard to fixation and stabilization.[8] Aligning McRae's line prevents superior and inferior tilting of head at the time of surgery.

Method for orienting the head in the three planes of space:

1. Coronal: In the coronal view, aligning the left and right optic foramina orients/registers the tilt of head. First adjusting the head, the axial plane was set through the center of the left and right optic foramina. Aligning these structures prevented left and right tilting of head (Fig. 3.).
2. Axial: In axial view, aligning the left and right foramina ovale orients/registers the rotation of the head. In axial view, adjusting the head, the coronal plane

was set through the center of left foramen ovale to the center of right foramen ovale. Aligning these structures prevents the rotation of head (Fig. 4.).

3. Sagittal: Two methods for orientation in the sagittal plane were examined. The first is to use foramen Cecum. After adjustment of head in the coronal and axial views, the sagittal view can be fixed using the foramen cecum. To do this, foramen cecum was selected to bisect the head to the intersection of coronal plane and axial plane. On this sagittal view, adjusting the head, the axial plane was set to overlap the McRae's plane denoted by a line touching the radiographic anterior border of foramen magnum (basion) to the posterior border of foramen magnum (opisthion). Aligning these structures oriented the superior and inferior position of the head (Fig. 5.).

After the head orientation has been established, the image should not change during subsequent quantitative analysis of the slice data derived from the CBCT image. One operator (GW) was trained and calibrated to identify 3D landmarks using the sagittal, coronal, and axial slices. Five anatomical structures, the left and right optic foramina, the left and right foramina ovale, foramen cecum were selected. The defined criteria were established for each landmark (Table I) and registered and recorded the center of these structures by the Invivo 5.0 software as numerical values for the X, Y, and Z coordinates respectively (Figs. 6-8). The digitized data were then exported to a Microsoft Excel spreadsheet (Microsoft Corporation, Redmond, WA). The identification of landmarks was repeated 3 times by the same operator at intervals of at least 3 weeks. The data for the study were derived from 90 samples, 3

times measurement for 30 samples. On each measurement, all 5 points had been located. Therefore, for each of 5 landmarks, 90 independently located estimates were available. The data-reduction problem was to relate 90 estimate for each landmark to each other in such a way that meaningful conclusion could be drawn.

Statistical analysis

Statistical analysis was performed using the Statistical Package for the Social Sciences software (version 17.0.1; SPSS, Inc., Chicago III). Unlike linear and angular measurements, coordinate data from different individuals cannot be meaningfully compared. Following the method established by Baumrind and Frantz, the dispersion of the landmarks in the x, y and z directions were estimated using the standard deviation as a measure of dispersion. [2] The mean of these standard deviations was calculated (measures of dispersion), the error of standard deviations (the estimating errors) were collected and calculated for each landmark and each coordinate. All voxel data were converted to millimeters by multiplication of 1 voxel times the voxel size of 0.38mm.

RESULTS

Results for the standard deviations in the x, y and z directions for all landmarks are given in table II and shown in Figs 9-12. All the measures of dispersion are less than 0.3mm, ranging from 0.078- 0.258mm in all directions (See Table II). Also the scatter plots demonstrate the distribution of error for all the landmarks in the X, Y, and Z directions. The variation of the estimates of foramen cecum is more along the horizontal (X) axis than vertical(Y) and anterior-posterior (Z) axes. The variations of the estimates of optic foramina are symmetrically distributed along the horizontal (X) axis, vertical (Y) and anterior-posterior (Z) axes. The variations of the estimates of foramina ovale are greater in the horizontal (X) axis compared to the vertical (Y) or anterior-posterior (Z) axes. Intra class correlation r=.99

DISCUSSION

The purpose of this study was to identify biologically relevant anatomic features that could be used for superimposition of longitudinal 3-D images in the same way longitudinal cephalograms are superimposed on cranial base landmarks. In 2-D superimposition, the American Board of Orthodontics (ABO) has adopted the following method for cranial base superimposition. They recommend registering "on the best fit of the anterior cranial base anatomy and center of sella turcica".[9] However, the stability of sella turcica over time has been questioned.[10-16] Even though all bones remodel over time, orthodontists and craniofacial biologists generally agree that the most stable structures are located in the anterior cranial base and sphenoid bone. In addition, bone surrounding nerve seems to be relatively stable. For example, Björk's metallic implant method has gained wide acceptance. Björk found that the mandibular nerve canal was surprisingly stable in its anatomic location within the mandible.[7, 16] Based on Björk we reasoned that some cranial nerves might also remain stable over time. We chose the optic foramina and foramina ovale because these structures are all located within the body of the sphenoid bone. Since bone cannot grow interstitially and there are no sutures or synchondroses within sphenoid bone after the first year of life, these foramina have limited biological ability for movement. Further, because brain size is almost complete at the age of 5 years even the length of the nerve canals is likely fixed.[14-15] These middle cranial fossa foramina represent the relative anatomically stable structures in the entire craniofacial complex.[17] Although all bony cranial structures undergo lifelong surface remodeling,

it is highly unlikely that the inner surface of nerve canals undergo dramatic changes on a routine basis since these changes would likely result in neural deficits in function. For superimposition purposes, it is favorable to superimpose on the landmarks which are in close proximity to the structures to be measured. Early in 1972, Ricketts suggested that foramina rotundum would be good landmarks for superimposition because these structures are close to the face and thus acceptable for measuring in the maxilla and mandible.[18] Our concept of using middle cranial fossa foramina is consistent with Ricketts'. However, comparing optic foramina with foramina rotundum, in present study, optic foramina were easier to identify and were relatively more level in coronal view, whereas foramina rotundum presented higher variance of vertical position in the coronal view.

Locating anatomic features in three space has been discussed in the literature. Houston in 1983 pointed out that many cephalometric landmarks in 2-D have been used for convenience of identification and reproducibility, rather than their anatomic validity.[4] And Bookstein mentioned that there is a lack of literature about suitable operational definitions for the 2-D traditional landmarks in the 3 coronal, sagittal, and axial plane.[19-20] Therefore, choosing anatomical relevant cranial structures used for the present study was not trivial. In Hodaie's study, the optic nerve included the prechiasmatic portion, the chiasm, the retrochiasmatic tract, and the optic radiation.[21] Anatomically, we selected the prechiasmatic portion of optic nerve to define the anatomic feature of interest. Radiographically, the prechiasmatic part of the nerve is the portion starting from chiasmatic groove and extending 3.8-4mm forward in the

sagittal and axial view. Berlis recommended that this was the most accurate way to view the optic foramina in the coronal plane.[22] Therefore, once the sagittal and axial views were adjusted properly, it was easy to register the center of optic foramina in coronal view. Also in Berlis' study, he suggested that it was optimal to locate the foramen ovale in the axial projection where it presented as a circular structure.[14] Radiographically, in the sagittal view, the middle portion of the opening of foramen ovale was located between the anterior wall located in the most posterior-superior part of lateral pterygoid process and the posterior wall presenting on the opposite side. In the coronal view, the middle portion of foramen ovale was located between the lateral and inner wall of the opening of the sphenoid bone. Once the sagittal and coronal views were adjusted properly, it was a simple matter to identify the center of foramina ovale in the axial plane. Our results confirmed Berlis' findings and demonstrated that these anatomic features could be reliably and accurately located in the population of interest to orthodontists.

Theoretically, head orientation should not be a major concern in 3-D superimposition for eliminating the errors of measurement.[14, 23] However, in the present study, cross-sectional 2-D slices were used instead of 3-D rendering in three planes for identification of landmarks. Since 3-D renderings are projected images and not actual surfaces, so registration on this projection causes more errors. Since single cross-sections of larger structures were viewed, small variations in head positioning led to large changes in the cross-section view.[24] Therefore, head orientation was still an important part of the present study. In 2-D cephalometric

studies, Broadbent's classic cepholostat used external cranial structures including the external auditory meatus, Frankfort horizontal plane, and nasion, to orientate the head.[1] In 3-D, some authors have used reference plans to establish a 3-D coordinate system. Park et al used facial structures, including left and right porions, orbitales, nasion and pogonion, to establish a 3-D coordinate system.[25] However the drawback of Park's method was that the facial landmarks selected to set up the 3-D coordinates undergo significant modification during growth and orthodontics treatment. Since 3-D provides clinicians with the ability to investigate the entire head slice by slice, in the present study, the optic foramina, the foramina ovale, basion, opisthion and foramen cecum were used to orientate the image. In the coronal view, aligning the left and right optic foramina fixed the left to right tilt of head. In the axial view, aligning the left and right foramina ovale fixed the rotation of the head. In the sagittal view, aligning basion and opisthion (McRae's line), fixed the superior and inferior tilt of the head. Initially, McRae's line was used first by neurologists to orient the head during intracranial procedures.[8] In 2-D, the head holder has been built into every cephalostat and oriented the head as is taken. This makes it easy to identify and register basion and opisthion on the cephalogram. However in 3-D, bisecting the head based on different landmarks results in different sagittal views. In the present study foramen cecum was used to bisect the head because anatomically foramen cecum was the center of anterior cranial base.[26] After the sagittal orientation fixed using foramen cecum, radiographically aligning basion and opisthion fixed the superior-inferior tilt of the head. Further, even though both McRae's line and

Frankfort horizontal line could be used to orient the head in the sagittal view, the use of a single midline structure like foramen cecum is more reliable than using bilateral structures like Frankfort plane and McRae's line. The selection of all of these structures was based on the fact that these internal cranial structures are not altered by orthodontic treatment and because cranial nerves go through these foramina. Among these foramina, the spinal cord, the biggest cranial nerve, passes through foramen magnum. Even though we did not test the stability of McRae's line in three dimensions, we did observe small distal changes in McRae's line. However, the distal movement of opisthion is parallel to McRae's line and doesn't change superior-inferior tilt of the head.

Most of the landmarks in the present study illustrated a circular envelope of error, indicating that the variation in landmark location was distributed evenly along all three axes. This result is consistent with Baumrind's description of the mental averaging process.[2] He tested several 2-D landmarks and found that each landmark has its own characteristic and usually noncircular envelope of error. If the landmark was formed by sharp folds, for example, the lower incisor edge, the estimation was relatively accurate and reliable. However, if the landmark points were characterized by gradual curves and surfaces, there was an oblong envelop of error. For example, A-point had twice the error in the y direction compared to x whereas ANS had more error along the x axis and less along the y axis. Interestingly, sella was among the points Baumrind found with a circular envelope of error. He reasoned that since the visual estimation of the center of the sella turcica requires a mental averaging process

the estimate is equally likely to vary in all directions.[2] Like sella, the landmarks used for this study required the operator to estimate the visual center of the feature. Our results were consistent with the 3-D landmark estimates previously reported by Lagravere. Lagravere scanned 10 dry skulls by CBCT to test the reliability and accuracy in locating several cranial base foramina for future use in establishing coordinate system.[17] He reported that intra-examiner reliability values for x, y, z coordinates were greater than 0.9. Mean measurement error differences obtained in the principal investigator's trials were less than 0.5mm.

As a first attempt this study focused on cross sectional images. The real value of superimposition is for longitudinal studies. Further studies are needed to determine if these landmarks are stable enough to allow useful serial superimposition on the cranial base.

Table I. Definition of the selected Landmarks for this study

Landmarks	*Anatomical structure*	*Axial view*	*Sagittal view*	*Coronal view*
Foramen cecum	notch at the lower end of the frontal crest and its articulation with the ethmoid bone	Middle point of the anterior-posterior width of the circle	Middle portion of the anterior posterior width of the canal	Middle portion of the canal in the coronal slice determined by the axial and sagittal views
Foramina ovale	situated in the posterior part of the sphenoid bone bilaterally and transmits the right/left mandibular division (CN V3) of the trigeminal nerve	Middle portion of right/left foramina in the axial view determined by the coronal and sagittal views	The middle portion between the anterior wall which locates in the most posterior-superior part of lateral pterygoid process and posterior wall which visibly locates in the opposite side	Middle portion between the lateral and inner wall of the opening of sphenoid bone bilaterally
Optic foramina	The opening to the optic canal which is the superior surface of the sphenoid bone bounded behind by a ridge. Transmits the right optic nerve (CN II)	the optic nerve on the right/left side starting from chiasmatic groove 4mm forward	4 mm forward from the chiasmatic groove	Middle portion of right/left optic foramina in the coronal view determined by the axial and sagittal views
McRae's line	A line drawn from the anterior margin of the foramen magnum (basion) to the posterior border (opisthion). Transmits spinal cord	Orientating the head in axial view based upon aligning the foramina ovale	After head orientation in coronal and axial views, the sagittal view was defined by setting the sagittal plane through the middle portion of foramen cecum. In this sagittal view, the anterior margin of the foramen magnum was defined as the basion and the posterior border of the foramen magnum was defined as the opisthion	Orientating the head in coronal view based upon aligning the optic foramina

Table II. Landmarks in X, Y, Z coordinate system

Landmarks	***X*** ***Mean ± SD(mm)***	***Y*** ***Mean ± SD(mm)***	***Z*** ***Mean ± SD(mm)***
Cecum	0.25 ± 0.10	0.14 ± 0.05	0.17 ± 0.06
Ovale Right	0.11 ± 0.07	0.12 ± 0.07	0.11 ± 0.06
Ovale Left	0.12 ± 0.09	0.13 ± 0.06	0.13 ± 0.09
Optic Right	0.13 ± 0.08	0.12 ± 0.07	0.08 ± 0.04
Optic Left	0.14 ± 0.07	0.11 ± 0.08	0.10 ± 0.05

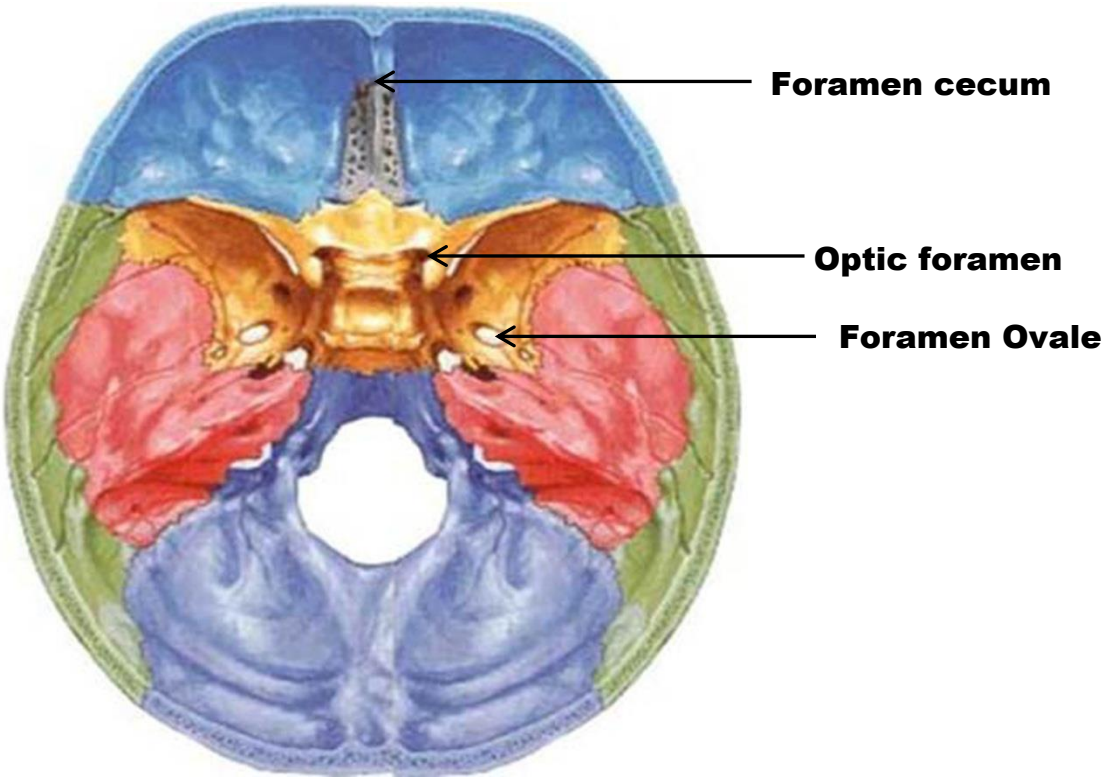


Fig. 1. Demonstration of biologically relevant anatomical structures

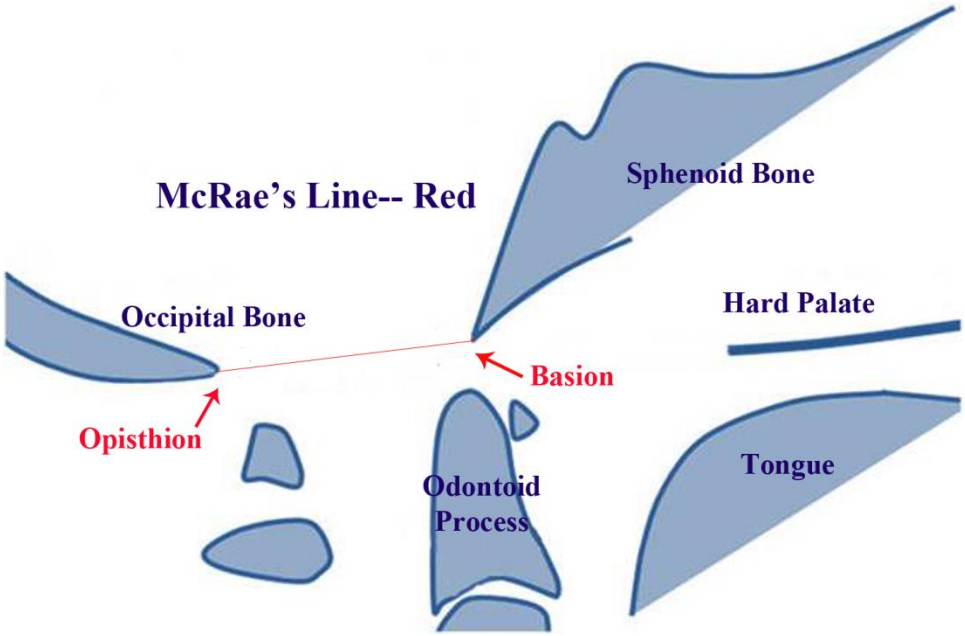


Fig. 2. McRae's Line is located in sagittal view and is defined as a line drawn from the anterior margin of the foramen magnum (basion) to the posterior border (opisthion).

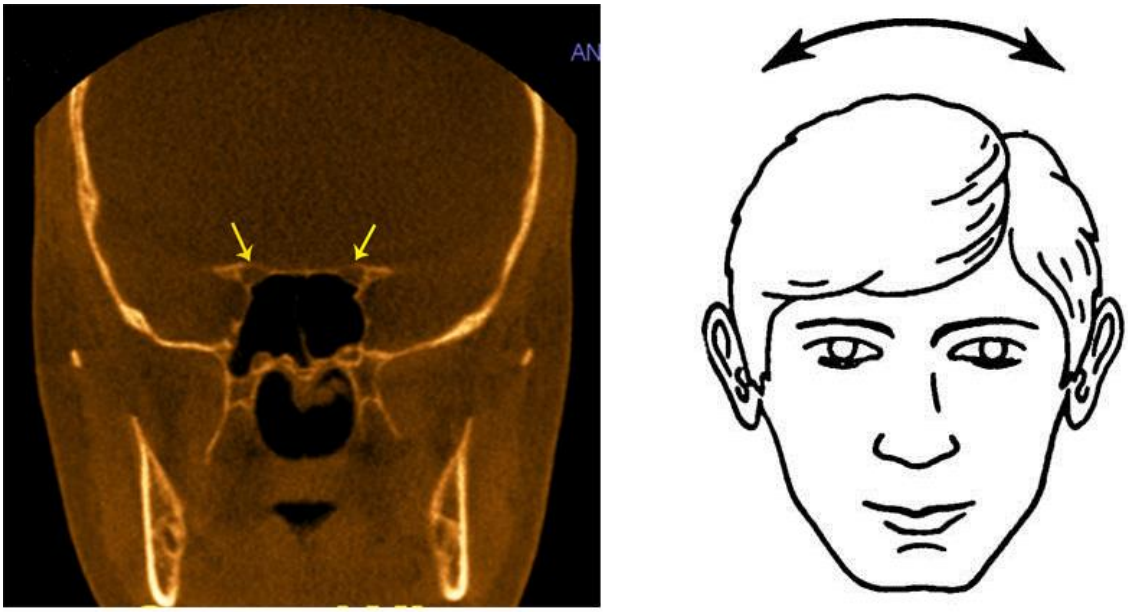


Fig. 3. Fixing/registering head position in the coronal view. **A,** The Optic foramina are in the coronal view (yellow arrows)**.** The axial plane was set through the center of the left and right optic foramina. **B,** Aligning these structures fixed the left and right tilting of the head.

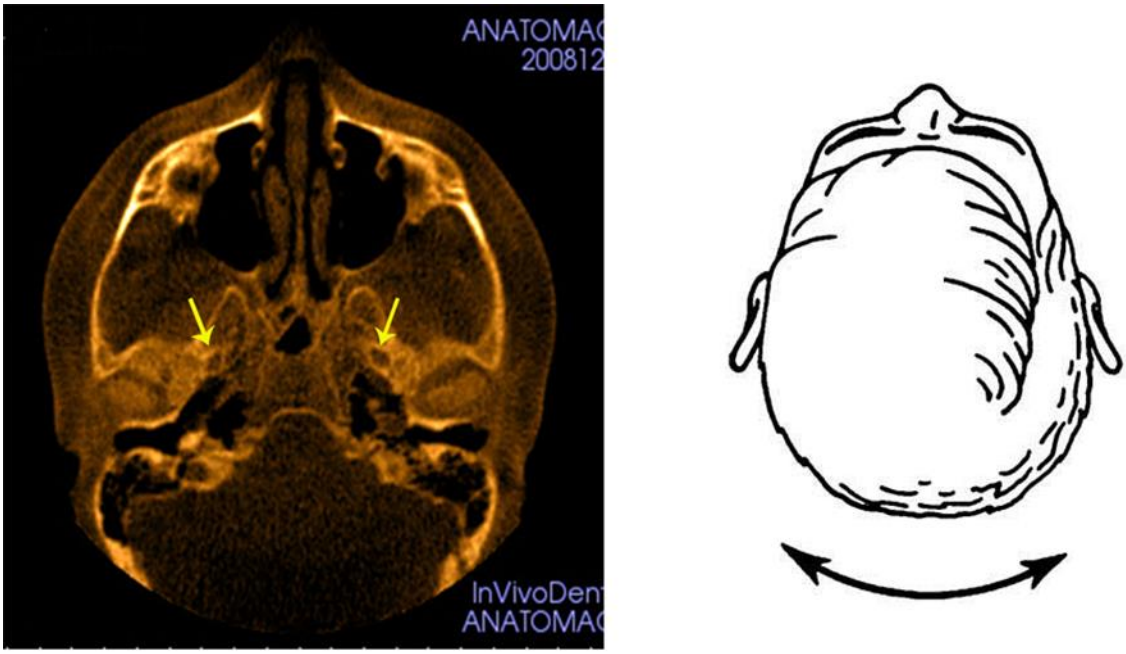


Fig. 4. Fixing/registering head position in the axial view. A, The foramina ovale are in the axial view (yellow arrows). The coronal plane was set through the center of the left and right foramina ovale. B, Aligning these structures fixed the left and right rotation of the head.

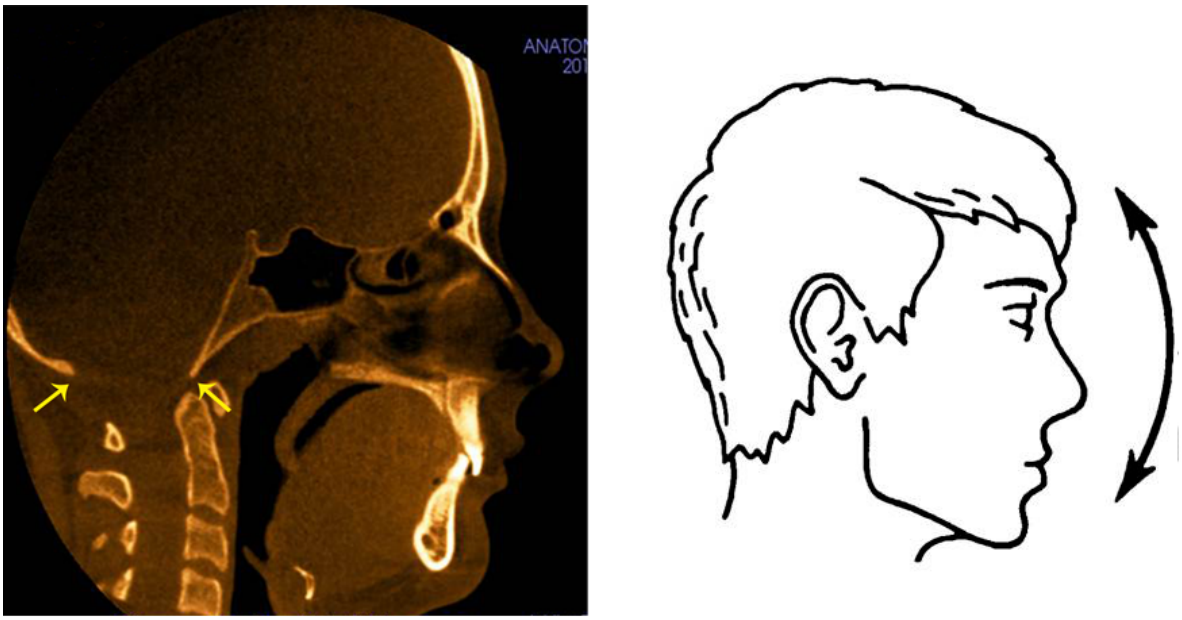


Fig. 5. Fixing/registering head position in the sagittal view. **A,** The axial plane was set to overlap the McRae's plane denoted by a line touching the radiographic anterior border of foramen magnum (basion, yellow arrow) to the posterior border of foramen magnum (opisthion, yellow arrow). **B,** Aligning these structures oriented the superior and inferior position of the head.

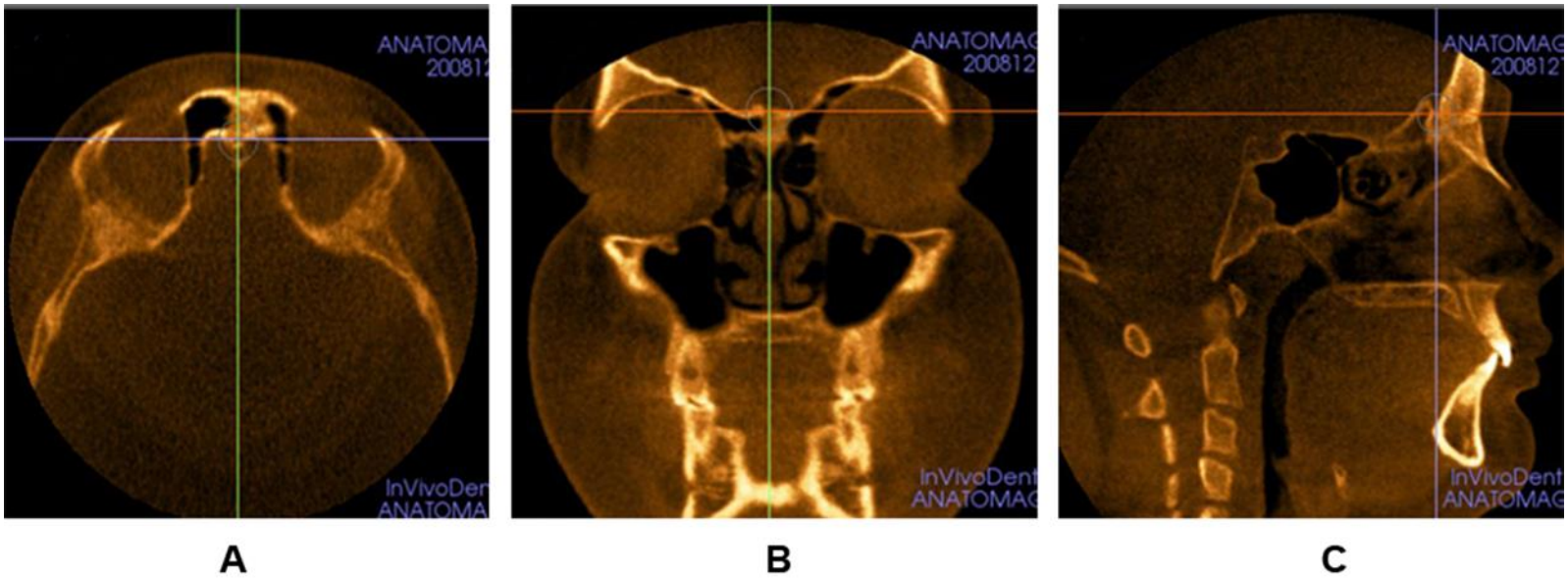


Fig. 6. Registering and recording the center of foramen cecum by the Invivo 5.0 software as numerical values for the X, Y, and Z coordinates respectively. **A,** Middle point of the anterior/ posterior width of the circle in axial view. **B,** Middle portion of the anterior/ posterior width of the canal in sagittal view. **C,** Middle portion of the canal in the coronal slice determined by the axial and sagittal views.

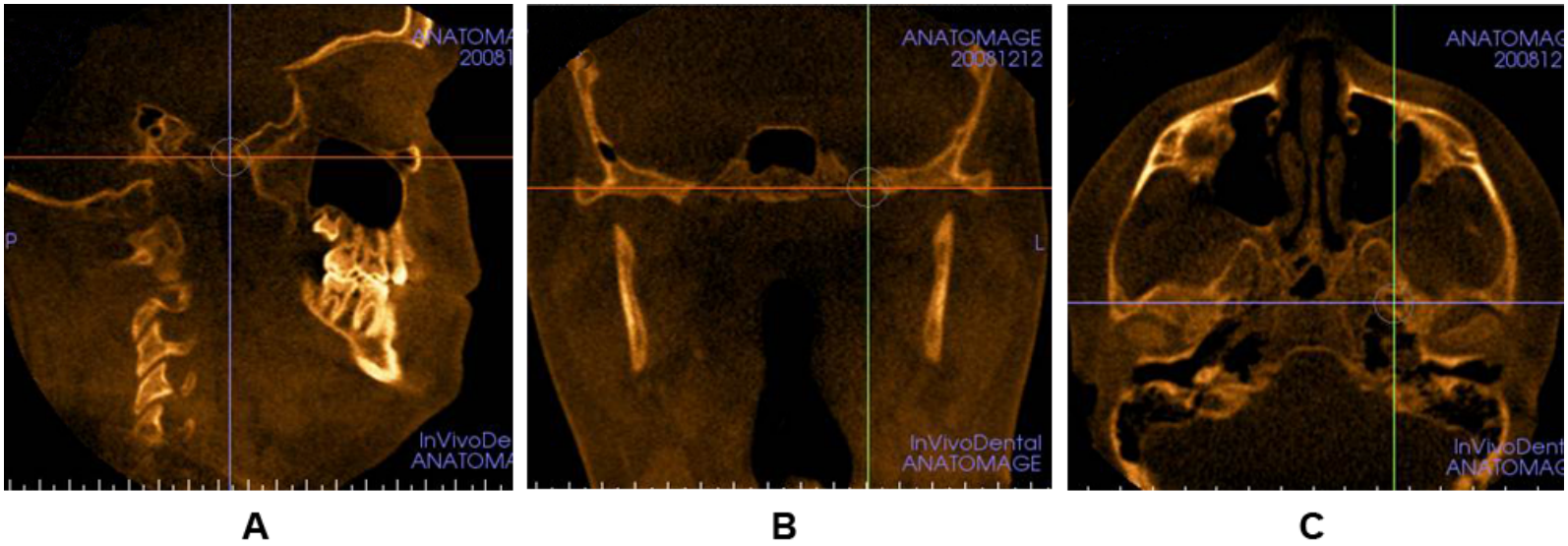


Fig. 7. Registering and recording the center of left foramen ovale by the Invivo 5.0 software as numerical values for the X, Y, and Z coordinates respectively. A, The middle portion between the anterior wall which locates in the most posterior-superior part of left lateral pterygoid process and posterior wall which visibly locates in the opposite side B, Middle portion between the lateral and inner wall of the opening of sphenoid bone on the left side C, Middle portion of left foramen in the axial view determined by the coronal and sagittal views.

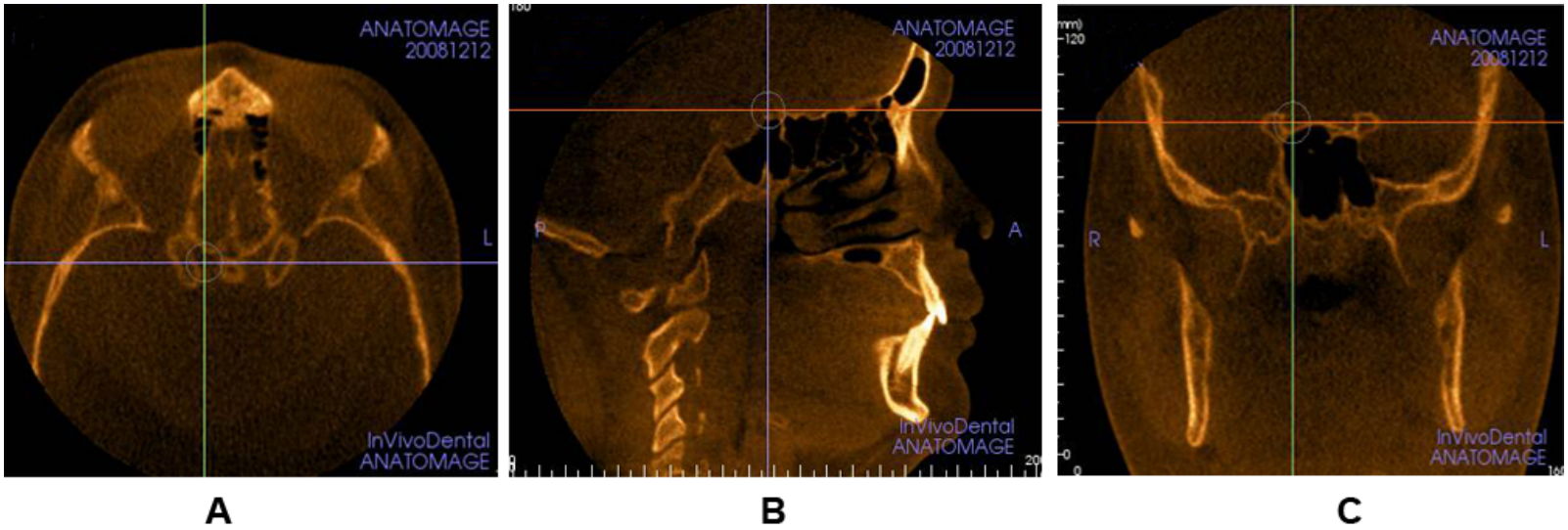


Fig. 8. Registering and recording the center of right optic foramen by the Invivo 5.0 software as numerical values for the X, Y, and Z coordinates respectively. A, the optic nerve on the right side starting from chiasmatic groove to 4mm forward. B, 4 mm forward from chiasmatic groove. C, Middle portion of left optic foramen in the coronal view determined by the axial and sagittal views.

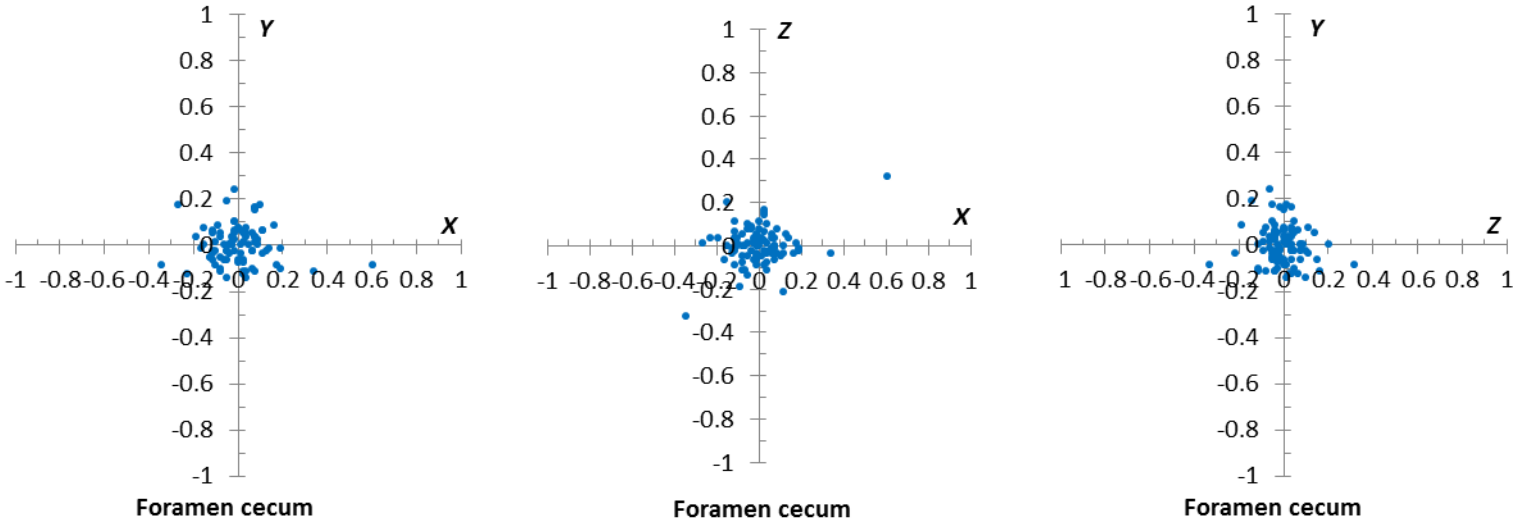


Fig. 9. Distribution of error for foramen cecum in the X, Y, and Z directions. The variation of the estimates of foramen cecum is more along the horizontal (X) axis than vertical(Y) and anterior-posterior (Z) axes.

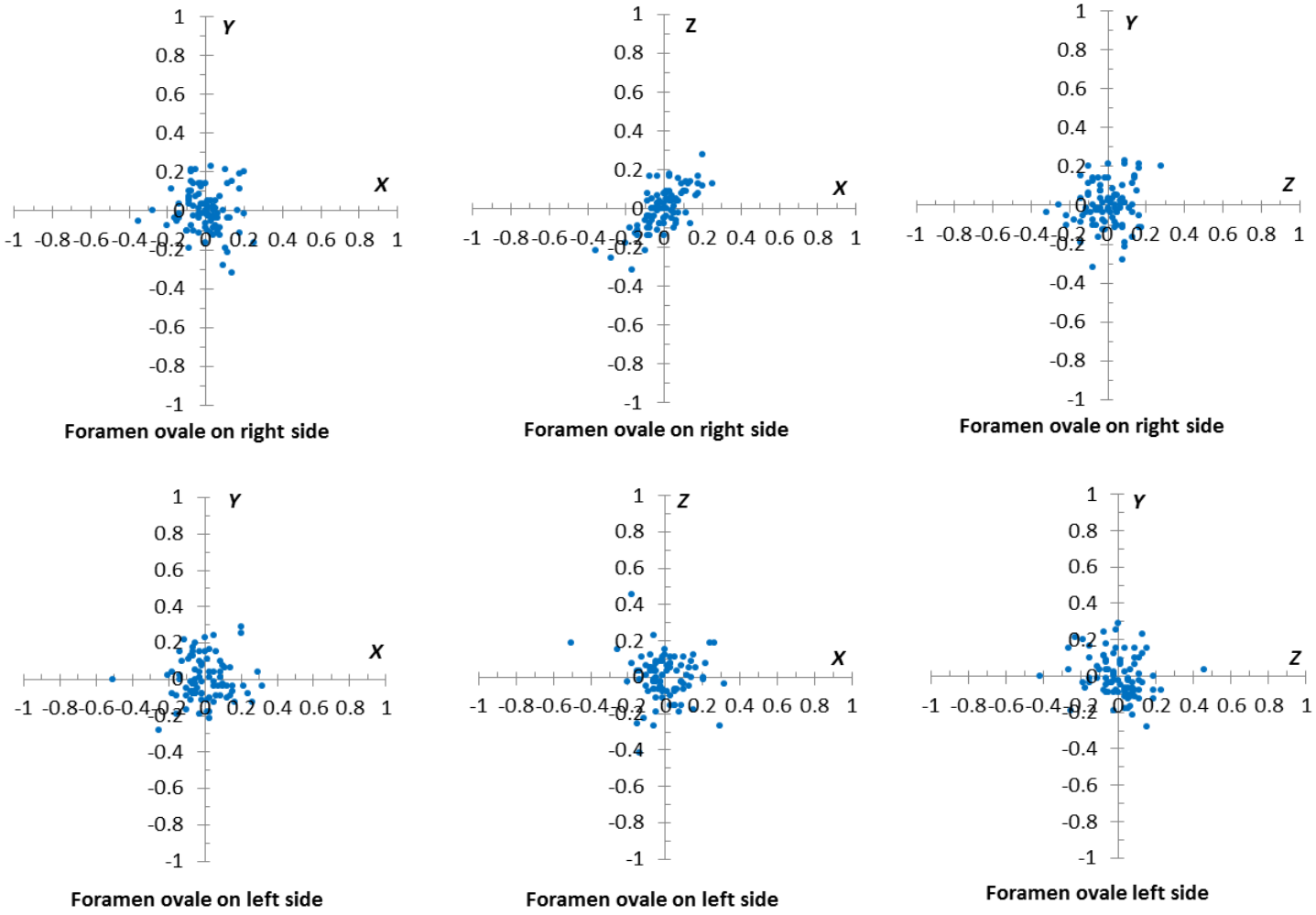


Fig. 10. Distribution of error for foramina ovale in the X, Y, and Z directions. The variations of the estimates of foramina ovale are greater in the horizontal(X) axis compared to the vertical(Y) or anterior-posterior (Z) axes.

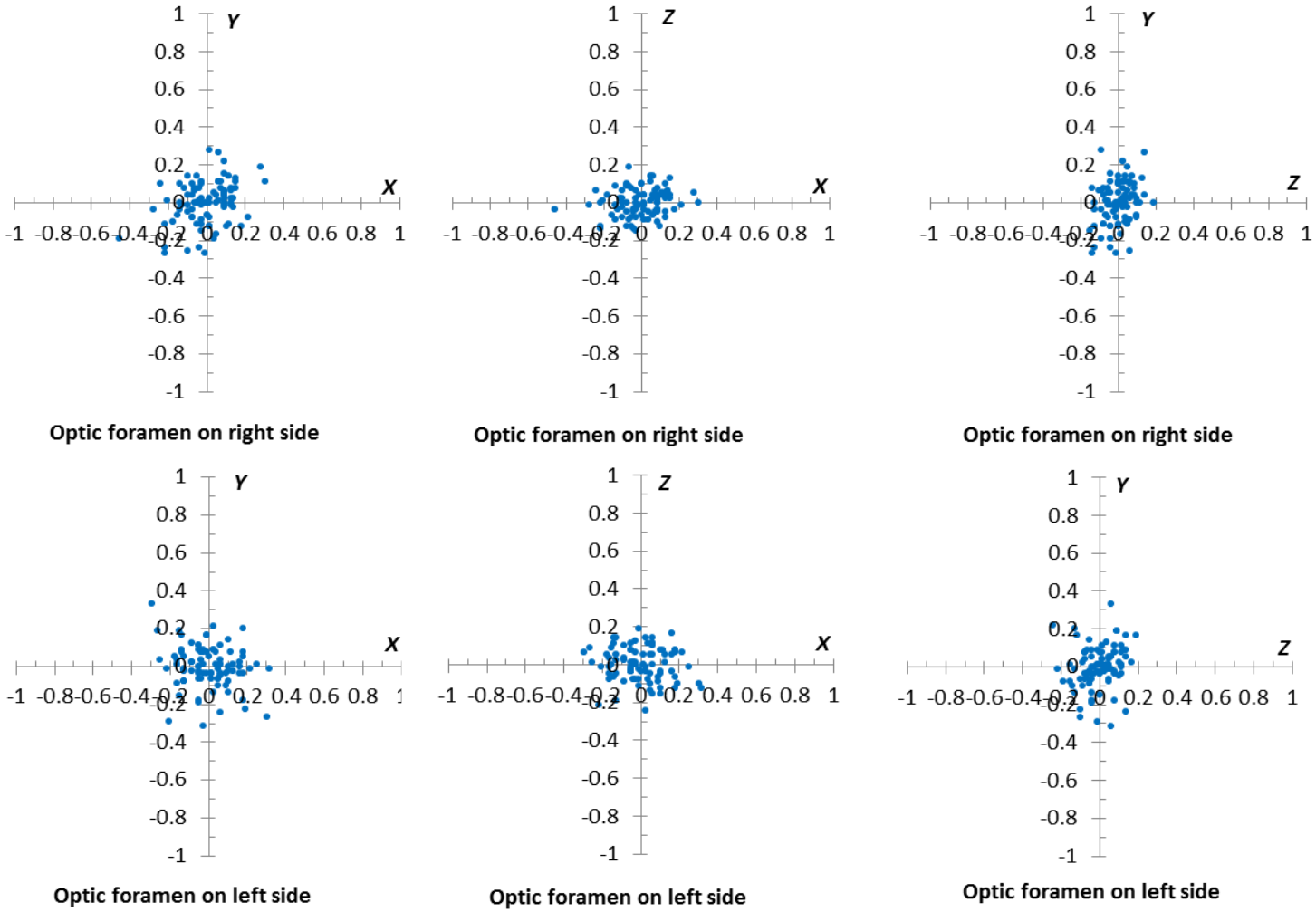


Fig. 11. Distribution of error for optic foramina in the X, Y, and Z directions. The variations of the estimates of optic foramina are symmetrically distributed along the horizontal(X) axis, vertical(Y) and anterior-posterior (Z) axes.

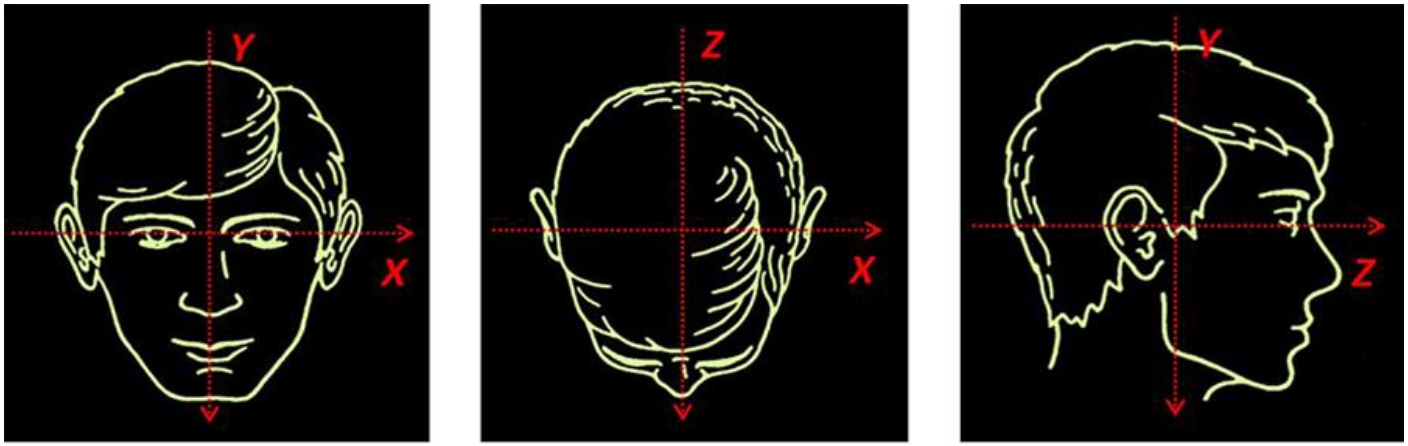


Fig. 12. Demonstrations on distribution of error in the X, Y, and Z directions by using coronal, axial and sagittal views.

REFERENCE

[1] Broadbent. "Broadbent BH 1931. A new x-ray technique and its application to orthodontia, the introduction of cephalometric radiography." Angle orthod. (Reprint 1981): 51:93-114.

[2] Baumrind, Sheldon and Robert C. Frantz. "The reliability of head film measurements:1. Landmark identification." American Journal of Orthodontics (1971): 111-127.

[3]Hans, M G. "Three-Dimensional imaging: The Case Western Reserve University Method." Semin Orthod (2001): 7:233-243.

[4] Houston, W.J.B. "Sources of error in measurements from cephalometric radiographs." European Journal of Orthodontics (1986): 149-151.

[5] Ahlqvist, J. "The effect of projection errors on cephalometric length measurements." European Journal of Orthodontics (1986): 141-148.

[6] Palomo, J. Martin. "clinical application of three-dimensional cranialfacial imaging in orthodontics." Journal Medical Science (2005): 269-278.

[7] Björk A, A. and V. Skieller . "Facial development and tooth eruption: An implant study at the age of puberty." Am J Orthod (1972): 62: 339-383.

[8] Goel, A. "Treatment of basilar invagination by atlantoaxial joint distraction and direct lateral mass fixation." J Neurosurg Spine (2004): 281-286.

[9] ABO. American Board of Orthodontics. Case report preparation: composite tracings. St Louis, Mo, 2007.

[10] Hans, Mark G and Donald Enlow. Essentials of Facial Growth. W.B. Saunders Company, 2008.

[11] Ricketts, RM. " New perspectives on orientation and their benefits to clinical orthodontics—part II." Angle Orthod (1976): 46:26–36.

[12] Baume, LJ. "Principles of cephalofacial development revealed by experimental biology." Am J Orthod (1961): 47:881–901.

[13] Coben , SE. "The spheno-occipital synchondrosis: the missing link between the profession's concept of craniofacial growth and orthodontic treatment." Am J Orthod

Dentofacial Orthop (1998): 114:709– 712; Discussion 713-704.

[14] Melsen, B. "The postnatal growth of the cranial base in Macaca rhesus analyzed by the implant method." Tandlaegebladet (1971): 75:1320–1329.

[15] Melsen, B. The cranial base: the postnatal development of the cranial base studied histologically on human autopsy material. Copenhagen: Arhus., 1974.

[16] Björk , A and V Skieller . "Normal and abnormal growth of the mandible. A synthesis of longitudinal cephalometric implant studies over a period of 25 years." . Eur J Orthod (1983): 5:1–46.

[17] Lagravère MO, "Cranial base foramen location accuracy and reliability in cone-beam computerized tomography." Am J Orthod Dentofacial Orthop. 2011 Mar;139(3):203-10.

[18] Ricketts RM. "The value of cephalometrics and computerized technology." Angle Orthod. 1972 Jul;42(3):179-99.

[19] Bookstein, Fred L. "Shape and the information in medical images: a decade of the morphometric synthesis." Computer Vision and Image Understanding (1997): 97-118.

[20] Bookstein , FL. "Morphometric tools for landmark data." Cambridge: Cambridge University Press (1991): 435.

[21] Hodaie, M. "In vivo visualization of cranial nerve pathways in humans using diffusion-based tractography." Neurosurgery (2010): 795-796.

[22] Berlis, A. "Direct and CT measurements of canals and foramina of the skull base." British Institute of Radiology (1992): 653-661.

[23] Badawi-Fayad. "Multi-detector row CT scanning in Paleoanthropology at various tube current settings and scanning mode." Surg Rodiol Anat (2005): 27(6):536-43.

[24]De Oliveira, Ana Emilia F. "Observer Reliability of Three-Dimensional Cephalometric Landmark Identification on Cone-Beam CT." Oral Surg Oral Med Oral Pathol Oral Radiol Endod (2009): 256-265.

[25] Park SH, Yu HS, Kim KD, Lee KJ, Baik HS. A proposal for a new analysis of craniofacial morphology by 3-dimensional computed tomography. Am J Orthod Dentofacial Orthop. 2006;129:600.23-34.

[26] Scott JH. The growth of cranial-facial skeleton. Ir J Med Sci. 1962 Jun;438:276-86.

APPENDIX 1

IRB Approval

Case Western Reserve University
Institutional Review Board

NOTICE OF EXEMPTION (#4)

Research involving the collection or study of existing data, documents, records, pathological specimens, or diagnostic specimens, if these sources are publicly available or if the information is recorded by the investigator in such a manner that subjects cannot be identified, directly or through identifiers linked to the subjects.

This protocol is exempt under the #4 category because this involves existing retrospective de-identified data.

Please note that this only applies to existing data.

Prospective data is NOT included in this exemption – i.e., De-identified pre-existing data to be collected on

05/14/2011 and after are NOT covered by this exemption.

Responsible Investigator: **J. Martin Palomo**
Department: **Dental Orthodontics**
IRB Protocol Number: **20110417**
Title: **Establishing a Superimposition Method to Compare Results in Pre- and Post-Treatment with CBCT: Part I: Stable Cranial-Based Landmarks for Three Dimensional Superimposition of CBCT**
Co-Investigator: **Rongning Wu**

Sample size calculation

Descriptive study

(Means of SD, SD of SD, and range of variables)

Confidence intervals= ± 0.5mm

Confidence level= 95%

Continuous variables.

SD= ± 0.64mm variability of X.Y. Z

Calculate sample size from Table 13 D (Descriptive study of a continuous variable)

W/S =Desired total width/SD

= 0.5/0.64

=0.8

Reading across from a standardized variable of 0.64mm and down from 95% confidence level, the required sample size is 25(30).

APPENDIX 2

Raw Data for all the anatomically based cranial landmarks:

Table 1.RAW DATA FOR FORAMEN CECUM COORDINATES.....59
Table 2. RAW DATA FOR LEFT FORAMEN OVALE COORDINATES.....60
Table 3. RAW DATA FOR RIGHT FORAMEN OVALE COORDINATES...61
Table 4. RAW DATA FOR LEFT OPTIC FORAMEN COORDINATES.....62
Table 5. RAW DATA FOR RIGHT OPTIC FORAMEN COORDINATES....63

Table 1. Raw data for the foramen cecum coordinates

Patients ID	Foramen cecum				Patients ID	Foramen cecum				Patients ID	Foramen cecum			
		X	Y	Z			X	Y	Z			X	Y	Z
WO84	1	95.8	55.9	128.8	***PU22***	1	97	68.5	134.4	***MC170***	1	102.5	57.2	130
	2	95.9	55.4	128.7		2	97.1	68.2	134.6		2	102.7	57	129.4
	3	95.4	55.8	128.9		3	97	68.4	134.6		3	102	57.1	130.5
BI61	1	95.3	51.4	116.9	***SE65***	1	101.1	62.1	131	***TO74***	1	100.3	57	140.4
	2	96.6	52.2	116.8		2	100.7	61.5	131.2		2	100.5	57.2	140
	3	95.2	51.7	116.7		3	101.2	61.9	131.1		3	100.4	56.8	140.2
SE83	1	101.2	55.7	147.2	***TO85***	1	99.4	51.1	135.4	***Hu104***	1	96.5	64.2	146.4
	2	100.9	55.3	146.9		2	100.3	51.1	136		2	95.7	64.6	146.4
	3	101.4	55.6	146.7		3	99.8	51.3	136.3		3	95.8	64.6	146.6
FL28	1	96.3	55.8	137.8	***ZD05***	1	100	60	134.3	***WA168***	1	97.7	49.7	142.3
	2	96.3	55.8	137.8		2	99.9	59.8	134.6		2	97.8	49.4	142
	3	96.5	55.8	137.7		3	100.2	60.3	134.3		3	98.5	49.5	142.1
HA403	1	94.3	53.4	152.6	***BA235***	1	97.8	59.3	151.6	***JA139***	1	97	70.5	135.4
	2	94.2	53.2	153.1		2	98.2	59	151.8		2	94.5	70.5	133.7
	3	94.5	53.2	152.8		3	98.1	58.9	151.9		3	94.7	71.2	134.6
HA359	1	97.5	71.1	145.4	***BE182***	1	106.3	55.2	134	***PA162***	1	97.6	125.4	142.5
	2	97.1	71.6	145.1		2	106.6	55.4	133.9		2	96.3	125.4	142.2
	3	97.2	71.5	145.3		3	106.3	55.3	134.3		3	97.3	125.8	142.3
KA123	1	103.5	54.6	135.7	***CR96***	1	99	58	139.5	***TO74***	1	100.8	119.5	132.2
	2	103.3	54.6	135.9		2	98.9	57	139.7		2	99.8	119	132.7
	3	103.1	54.6	135.8		3	99.2	57.1	139.8		3	99	119.7	131.9
LO87	1	97.7	55.5	146	***WI298***	1	98	55.7	138.1	***MC170***	1	98.2	114.9	127.9
	2	97.3	55.6	145.5		2	97.3	122.7	151.2		2	97.4	114.9	128
	3	97.1	55.6	145.9		3	97.3	123.1	151.5		3	97.7	114.5	128.1
MI197	1	100.6	68.2	140.1	***GO128***	1	104.7	63.4	157.3	***PA162***	1	97.3	57.2	134.3
	2	100.5	68	140.3		2	104.5	62.9	156.8		2	97.5	56.5	134.6
	3	100.6	68.7	140.3		3	104.9	63.3	156.9		3	97.5	56.4	135.1
NE19	1	95.4	58	145.7	***IL3***	1	98.8	62.1	163.9	***FE49***	1	95.2	68.1	167
	2	95.8	58.2	145.1		2	98.9	62	163.8		2	95.6	67.9	167.2
	3	95.9	58.1	145.4		3	99.5	62.4	163.7		3	95.8	68.7	166.9

Table 2. Raw data for the right foramen ovale coordinates

Patients ID	Foramen ovale right				Patients ID	Foramen ovale right				Patients ID	Foramen ovale right			
		X	Y	Z			X	Y	Z			X	Y	Z
WO84	1	71	115.6	97.5	***FL28***	1	74.2	115.9	109.3	***HA420***	1	70.6	117.4	110.2
	2	70.4	115.2	97.7		2	74.1	115.7	109.3		2	71.2	116.3	109.8
	3	70.9	115.1	97.3		3	73.9	116.1	109.9		3	70.7	117.7	110
BI61	1	70.2	111.9	86.8	***HA403***	1	71.2	105.8	118	***KA27***	1	70.3	115.1	107.4
	2	71	112	87.4		2	71	105.8	118.3		2	70.7	114.6	107.6
	3	70.8	111.8	87		3	71.4	105.7	117.9		3	70.5	114.8	107.5
SE83	1	70.4	113	111.4	***HA359***	1	71.1	121.4	101.2	***PI70***	1	76.2	113.2	114.9
	2	70.4	112.8	110.7		2	71	121.7	100.9		2	76.6	112.2	115
	3	70.3	113.4	111.1		3	71.1	120.9	100.6		3	75	112.5	114.1
KA123	1	75.8	111.3	107.6	***NE19***	1	73.7	117.3	114.4	***HU104***	1	76	116.6	109.3
	2	75.6	111.3	107.4		2	72.9	116.6	113.2		2	76.2	117.2	109.7
	3	75.7	111.4	107.3		3	73.4	116.8	114.5		3	75.5	116.7	109
LO87	1	73	115.2	110.6	***PU22***	1	74.7	120.3	101	***WA168***	1	71.9	104.4	106.9
	2	72.3	115.3	110.8		2	74.8	120.4	101.8		2	73.1	104.9	108
	3	72.1	115.2	110.7		3	74.4	120.6	101.3		3	72.9	103.9	107.8
MI197	1	73.9	120.5	99	***SE65***	1	73.9	110.9	100.8	***JA139***	1	72.4	114.5	98.3
	2	74	120	98.4		2	73.8	110.5	100.2		2	72.1	115.6	97.9
	3	74.4	119.8	98.3		3	73.7	110.9	101		3	72	115.6	98.1
TO85	1	73.4	109.5	108.1	***BE182***	1	74.1	109.8	104.3	***TO74***	1	73.6	117.7	111.6
	2	73.1	110.2	108.5		2	74	110.5	104.4		2	72.8	116.9	110.3
	3	73.3	109.8	108.5		3	73.7	109.4	103.8		3	72.8	116.9	110.7
ZD05	1	73.8	113.8	100.2	***CR96***	1	73.8	112.3	110	***PA162***	1	74.5	123.6	118.2
	2	73.2	113.7	100.1		2	73.5	112.2	109.7		2	74.8	123.1	118.4
	3	74.2	114.2	100.4		3	74.3	111.8	110.2		3	74.6	123.5	118.3
BA235	1	69.1	119.2	126.5	***WI298***	1	70.3	111.1	107.7	***MC170***	1	74.9	115.4	106.6
	2	69.2	119.1	126.4		2	70.3	110.9	107.7		2	75.1	115.1	106.4
	3	69	119	126		3	71	111	108		3	75	115	106.6
GO128	1	75.6	116.1	119.7	***FE49***	1	70.7	118.8	124.3	***IL3***	1	72	121.2	116.1
	2	75.5	116.6	119.4		2	70.8	118.4	124		2	72.2	121.1	116.4
	3	76	115.5	119.8		3	70.4	118.8	124.3		3	71.8	122	116.9

Table 3. Raw data for the left foramen ovale coordinates

Patients ID	Foramen ovale left				Patients ID	Foramen ovale left				Patients ID	Foramen ovale left			
		X	Y	Z			X	Y	Z			X	Y	Z
WO84	1	122.4	117.5	100	***FL28***	1	122.2	113.2	109.6	***WA168***	1	124.2	108.7	107.8
	2	121.2	116.8	100.3		2	122.2	113.4	109.3		2	123.9	108.6	108.4
	3	121.1	117	100.3		3	122.6	113.6	109.2		3	124.6	109.1	108.1
BI61	1	118.8	112.7	87.1	***HA403***	1	121.2	103.7	117	***JA139***	1	118.8	115.6	99
	2	119.2	112.8	87.3		2	121.5	103.8	116.6		2	118	114.5	99.4
	3	119.5	112.9	87		3	121.1	104	116.7		3	118	114.7	98.9
SE83	1	126.1	112.1	109	***HA359***	1	125	119.9	100.1	***KA27***	1	123.6	112	105.5
	2	126	112.1	108		2	124.8	119.3	100.4		2	123.2	112.7	106.4
	3	126.3	112.7	110.3		3	125	119.2	100.3		3	122.8	111.6	106.7
KA123	1	127.7	112.9	106.9	***NE19***	1	123.7	115.5	113.9	***PI70***	1	128.9	113.2	114.6
	2	127.6	112.9	107.5		2	124.3	114.9	113.1		2	129.1	112.7	115
	3	128.1	112.8	107.5		3	123.7	116	113.7		3	127	112.8	113.9
LO87	1	120.6	116	111.9	***PU22***	1	121.8	118.3	101.1	***HU104***	1	121.9	117.1	110.7
	2	120.4	115.6	111.9		2	121.8	118.8	101		2	121.6	117.4	110.9
	3	119.7	115.9	112.1		3	121.9	118.7	100.3		3	121.4	116.9	110.6
MI197	1	128.2	119.2	98.2	***SE65***	1	120.9	115	99.9	***HA420***	1	120	120.4	107.7
	2	128.2	118.7	98		2	120.6	114.6	99.1		2	119.6	119.8	108.3
	3	128	118.7	97.7		3	120.5	115.2	99.5		3	119.8	119.8	108.6
TO85	1	122.4	111.8	107.2	***BE182***	1	126.1	110.5	101.7	***MC170***	1	123.9	119.2	107
	2	122.9	111.8	107.4		2	125.9	110.7	101.8		2	124	119.8	106.8
	3	123	111.5	106.7		3	125.9	111.1	102.1		3	124.6	119	107.1
ZD05	1	119.9	115.3	98.2	***CR96***	1	124.8	112.2	108	***TO74***	1	127.9	117.2	109.2
	2	120.7	116	97.9		2	124.4	112.4	107.8		2	127.7	117.5	109.2
	3	121.1	116.8	98		3	124.5	112.7	107.8		3	128	118.3	108.9
BA235	1	121	121.3	123.6	***WI298***	1	116.9	111.4	107.7	***IL3***	1	125	122.3	115.3
	2	120.5	120.7	123.5		2	117.3	112.1	107.6		2	124.7	122.1	115.3
	3	120.5	121.6	123.9		3	116.9	112.1	107.4		3	125.8	122.8	114.3
GO128	1	128	118.5	118.8	***FE49***	1	122.2	116.8	124.3	***PA162***	1	122	127.3	117.9
	2	127.9	118.5	119.1		2	123.3	116.7	123.4		2	121.8	127.5	118.7
	3	127.9	118.7	118.5		3	122.3	117.6	124.6		3	122.1	127.4	117.7

Table 4. Raw data for the right optic foramen coordinates

Patients ID	Optic foramen Right				Patients ID	Optic foramen Right				Patients ID	Optic foramen Right			
		X	Y	Z			X	Y	Z			X	Y	Z
WO84	1	84.1	99.2	119.4	***FL28***	1	87.7	101.4	132.8	***TO85***	1	88.6	102	122.1
	2	85.1	100	119.8		2	86.9	100.2	132.4		2	88.3	101.3	121.6
	3	85	99.9	119.7		3	87.8	100.9	133		3	88.4	101.6	122.2
BI61	1	84.2	97.1	107.7	***HA403***	1	84.2	93.2	141.9	***ZD05***	1	87.7	100.8	122.9
	2	84.3	96.9	107.8		2	83.8	93.3	142.1		2	87.5	100.4	122.6
	3	83.8	96.5	108.3		3	83.6	93.2	142.1		3	87.6	100.1	122.6
SE83	1	90.1	98.8	139.8	***HA359***	1	88.6	110.8	125.3	***BA235***	1	86.8	105.9	147.1
	2	90.7	98.9	139.8		2	89	111.2	124.7		2	86.6	105.4	147
	3	90.6	99	139.3		3	88.7	110.4	124.4		3	87.4	105.5	147
KA123	1	91	96.8	127.7	***NE19***	1	86.7	100	134.3	***GO128***	1	92	103.1	141.1
	2	91.9	97.1	127.6		2	86.7	100	134.4		2	92	102.5	141.2
	3	90.6	95.9	127.1		3	86	99.6	134.5		3	91.9	103.9	140.8
LO87	1	88.6	100.3	133.1	***PU22***	1	87.1	108.2	125.7	***IL3***	1	85.6	104	143.8
	2	87.8	99.8	132.6		2	87.4	108.7	125.7		2	85.1	103.4	143.5
	3	88.2	99.8	132.6		3	87.6	108.6	126.1		3	85.4	103.7	143.8
MI197	1	90.3	108	124.5	***SE65***	1	88.6	102	122.1	***PA162***	1	91.1	111.8	142.5
	2	90.9	108.4	124.9		2	88.3	101.3	121.6		2	90.8	111.5	142.2
	3	90.3	107.9	125.1		3	88.4	101.6	122.2		3	90.7	111.9	142.5
BE182	1	90.3	92.5	123.5	***CR96***	1	88.6	98	130.7	***TO74***	1	92.3	103.6	133.5
	2	90.7	91.5	123.3		2	88.2	96.6	130.3		2	92.2	103.5	133.9
	3	89.4	92.4	123.4		3	88.1	97.3	130		3	91.4	103.1	133.7
WI298	1	87.2	99.5	130.8	***FE49***	1	87.8	112.6	153	***MC170***	1	91.2	103.4	126.6
	2	87	99.1	130.6		2	87.3	112.6	153.1		2	90.6	103.5	127
	3	86.9	99.7	130.7		3	87.6	112.3	152.7		3	91.1	102.8	126.6
HU104	1	87	103.5	132.6	***HA420***	1	84.8	100.5	130.6	***WA168***	1	86.2	92.8	130
	2	87.2	103.7	133.1		2	84.6	100.2	130.3		2	85.9	92.8	130.1
	3	87.4	103.9	132.9		3	84.6	100.3	130.5		3	85.5	92.8	130.2
KA27	1	86.4	100.7	133.3	***PI70***	1	89.3	97.9	137.2	***JA139***	1	88.5	107.7	124.6
	2	85.8	100.4	133.1		2	89.1	98	136.7		2	90.5	108.5	124.5
	3	86	101	133.1		3	88.4	98	136.8		3	90.1	108.4	124.5

Table 5. Raw data for the left optic foramen coordinates

Patients ID	Optic foramen Left				Patients ID	Optic foramen Left				Patients ID	Optic foramen Left			
		X	Y	Z			X	Y	Z			X	Y	Z
WO84	1	107.5	100	120.5	***FL28***	1	107.6	100.3	132.9	***TO85***	1	110.2	95.6	128.5
	2	106.9	100.7	121		2	108.5	99.2	132.4		2	111.3	95.3	128.6
	3	106.7	100.8	121		3	107.9	99.9	132.7		3	111.1	95.2	128.3
BI61	1	105.8	97.4	107.9	***HA403***	1	106.2	92.3	141.4	***ZD05***	1	106.9	101.4	122.1
	2	105.9	97.2	107.8		2	106.3	92.2	141.4		2	107.7	101.3	121.7
	3	106.1	97	108.3		3	106.5	92.4	141.6		3	107.2	101.2	121.6
SE83	1	110.8	98.5	138.9	***HA359***	1	108.8	110.2	125	***BA235***	1	106.8	107	145.5
	2	109.2	99.4	139		2	109.2	110.3	124.6		2	105.8	107.4	145.8
	3	109.9	97.7	138.2		3	109.4	109.7	124.3		3	106.4	106.9	146.2
KA123	1	110.7	97.4	127.4	***NE19***	1	109.3	99.2	134.1	***GO128***	1	113.1	104	140.7
	2	110.1	97.7	127.6		2	108.5	99.3	134.4		2	113.3	103.3	141.1
	3	111.6	96.5	127.1		3	108.4	99.2	134.1		3	112.6	104.5	140.9
LO87	1	107.3	100.6	133.6	***PU22***	1	109.2	107.3	125.8	***IL3***	1	108.1	104.3	142
	2	107.9	99.9	133		2	108.7	108.2	125.4		2	109.1	103.8	143
	3	107.8	100	133.1		3	108.3	107.8	125.7		3	108.8	104.1	142.7
MI197	1	111.4	107.4	124.2	***SE65***	1	110.2	103.9	121.6	***PA162***	1	105.9	112.9	142.4
	2	111	107.9	124.8		2	110.6	103.2	121.1		2	106.1	112.9	142.3
	3	111	107.5	124.8		3	110.2	103.6	121.5		3	106	113.1	142.3
BE182	1	117	93.3	122.8	***CR96***	1	110.7	98	129.8	***TO74***	1	110	103.4	132.7
	2	116.4	93	122.4		2	111.1	96.7	129.9		2	110	103.7	133.6
	3	117.1	93	122.4		3	111	97.7	128.9		3	109.9	103.6	133
WI298	1	105.4	99.6	130.8	***FE49***	1	105.3	111.6	153	***MC170***	1	108.9	104.8	126.7
	2	105.6	99.5	130.1		2	105.1	111.8	152.8		2	108.3	105.2	127.2
	3	105.4	100.1	130.5		3	105	111.9	152.9		3	109.1	104.3	126.8
HU104	1	107.7	103.7	133.2	***HA420***	1	106.4	101.8	129.5	***WA168***	1	106.3	94.5	130.3
	2	107.4	103.7	133.6		2	106.6	101.8	129.6		2	107.2	94.4	130.3
	3	107	104	133.6		3	107.2	101.2	129.8		3	106.1	94.8	130.3
KA27	1	108.9	99.4	132.4	***PI70***	1	111.4	97.9	137.1	***JA139***	1	104.3	108.1	124.9
	2	108.3	99.5	132.6		2	111.7	98	136.7		2	104.4	108.2	125
	3	108.1	99.4	132.7		3	111.8	98.1	136.6		3	103.7	108.2	124.7